Thermal Performance Of Energy Retaining Walls In Hot-Dominant Climates: Experimental Evaluation In Unsaturated Brazilian Soil

Bruna Ruiz Carvalho Tosin, Cristina De Hollanda Cavalcanti Tsuha, Fleur Loveridge, Jose Antonio Schiavon, Aakash Gupta

Accepted for publication in Energy and Buildings 28th November 2025. Available online 6th December 2025. DOI: HTTPS://DOI.ORG/10.1016/J.ENBUILD.2025.116803

ABSTRACT

Ground source heat pump (GSHP) systems are widely adopted across many countries as efficient solutions for space heating and cooling, harnessing shallow geothermal energy—a renewable and low-carbon resource. In Brazil, where a substantial share of electricity consumption is linked to buildings, particularly due to air conditioning in the predominantly warm tropical climate, the integration of earth-retaining structures as ground heat exchangers—known as energy walls—presents a promising and cost-effective alternative to improve GSHP performance. A significant portion of Brazil's landmass consists of unsaturated soils, where seasonal transitions between dry and rainy periods result in fluctuating groundwater levels and degrees of saturation. These changes affect essential ground thermal properties, such as thermal conductivity, and must be considered in the design of geothermal systems. This study presents preliminary findings from the first field investigation on energy retaining walls in Brazil, conducted at a representative tropical unsaturated soil site at the University of São Paulo in São Carlos. Two thermal performance tests (TPTs) were conducted during the rainy summer season—a period of increased cooling demand —on concrete wall panels embedded in unsaturated lateritic clayey sand. The objective of the tests was to assess the thermal performance of the lower section of an energy wall in contact with unsaturated soil on both sides, and to examine how different operating conditions (intermittent versus continuous operation) influence its performance in building cooling applications. Temperature sensors installed within the wall and surrounding soil recorded thermal variations throughout the heating and recovery phases. In addition, both numerical and analytical models were validated against the experimental results, exhibiting good agreement and demonstrating their suitability for long-term predictions. The present results offer valuable insights for the future design and implementation of energy retaining walls in tropical unsaturated soil environments.

Key words: Energy retaining walls, Unsaturated soils, Hot-dominant climates, Ground source heat pump, Shallow geothermal energy, Building thermal comfort.

1. Introduction

The increasing adoption of renewable energy sources is a key component of sustainable technologies for controlling indoor building temperatures. In Brazil, residential electricity consumption for air conditioning reached 18.7 TWh in 2017 and is projected to increase to 48.5 TWh by 2035 [1]. As an alternative, thermoactive geostructures employ underground structures such as deep foundations, retaining walls, and tunnels as ground heat exchangers in ground source heat pump (GSHP) systems, enabling the use of shallow geothermal energy for space heating and cooling. Heat exchange is achieved by circulating a fluid, typically water, through pipes embedded in underground structural elements, which can significantly reduce the overall cost of GSHP systems [2]. This solution is both economically viable and easier to implement compared to the installation of deep boreholes as ground heat exchangers.

The Brazilian National Energy Plan 2050 (PNE2050) identifies shallow geothermal systems as a promising technology within the national energy strategy [3]. However, seasonal variations in ground saturation levels in Brazil affect the soil's thermal properties over time, potentially leading to inaccurate estimations—either under- or overestimations—of the outlet fluid temperature from thermoactive geostructures. One of the main challenges associated with these systems arises from their installation in unsaturated soils within regions characterized by high cooling demand. In such conditions, unbalanced thermal loads can lead to a gradual increase in ground temperature, reducing the efficiency of ground source heat pump (GSHP) systems [4]. Over time, continuous heat injection into the ground can degrade system performance. This issue is particularly critical in buildings with dominant cooling demand, where retaining walls serving as ground heat exchangers in GSHP systems (known as energy walls) are installed in unsaturated soils. In such conditions, limited heat transfer and the absence of groundwater hinder the dissipation of accumulated heat. To investigate this problem, short-term thermal performance tests (TPTs) were conducted on energy wall panels constructed to simulate a building basement (Figure 1). These panels, instrumented with temperature sensors, were tested under both intermittent and continuous operation modes for comparison.

The primary characteristic of the Thermal Performance Test (TPT) is its ability to maintain a nearly constant inlet temperature of the heat exchanger fluid throughout the test duration. As noted by [5], temperature-controlled testing is gaining interest because heat pump manufacturers typically define the system's coefficient

of performance (COP) based on the fluid's inlet temperature to the heat pump (i.e., the outlet temperature from an energy retaining wall). As an in-situ field method, the TPT enables the assessment of energy walls' thermal performance under realistic conditions that closely replicate heat pump operation in buildings, where maintaining a specific target temperature on the user side is generally required [6].

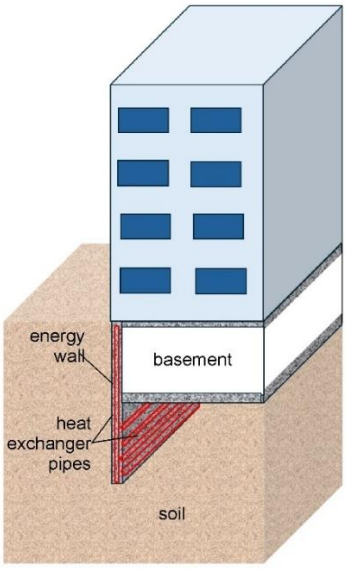

Figure 1. Illustration of an energy retaining wall integrated into a typical building structure.

The thermal performance of energy walls has primarily been studied through numerical simulations [7,8]. However, only a limited number of field tests have been conducted and documented, and even fewer analytical models have been developed for thermal analysis. One of the earliest implementations dates to 1996, when the first energy wall systems were installed in Switzerland and Austria, with an expected annual energy output of 175 MWh for heating and 437 MWh for cooling [9]. A short-term field test at the Shanghai Museum of Natural History in China, conducted by [10], investigated the effects of heat exchanger configuration, fluid flow rate, inlet temperature, and operational modes (continuous and intermittent) on energy wall performance. The study reported average heat exchange rates of 82.8 W/m for intermittent operation and 72.1 W/m for continuous operation, measured per meter of buried heat exchanger.

Kürten et al. [11] developed a semi-analytical model based on thermal resistances to reduce computation times compared to full numerical simulations. They also conducted a large-scale laboratory experiment on a concrete panel using two pipe configurations and a constant inlet temperature, reporting heat fluxes ranging from 36 to 150 W/m² in cooling mode. More recently, Baralis and Barla [6] proposed a novel geothermal wall

system designed for ease of installation, lower upfront costs, and suitability for retrofitting existing buildings. Their tests reported heat exchange rates of 18.6 W/m² for heating (heat extraction from the soil) and 68 W/m² for cooling (heat injection into the soil), with operation durations ranging from 48.1 to 1502.6 hours.

Despite recent advancements, most studies on thermoactive geostructures have been conducted in temperate climates and often overlook the effects of thermal load imbalances. Emerging research has begun to address energy piles in hot-dominated regions—particularly for cooling applications—to support climate-adapted design practices [12–17]. However, none of these studies have included full-scale field testing of energy retaining walls in tropical climates, a critical step toward developing reliable and effective design strategies for hot and humid environments. While practical applications have primarily focused on energy piles, the use of embedded retaining walls as both structural elements and ground heat exchangers is increasingly attracting attention. Nonetheless, the lack of field testing for these systems limits the ability to accurately assess their energy potential without relying heavily on full-scale numerical simulations.

To address these research gaps, the present study, based on field tests, aims to evaluate the thermal performance of the lower section of an energy wall in contact with unsaturated tropical soil on both sides. This study provides key insights for the design and evaluation of energy walls in hot-dominated climates installed in unsaturated soils. The main objectives of this paper are to:

a) Present and interpret field test results to evaluate the impact of different operation modes of GSHP systems (continuous and intermittent) on the heat exchange response between the wall and surrounding unsaturated soil under hot-climate conditions.
b) Examine the soil's thermal recovery capacity following a period of continuous heat rejection in the ground.
c) Assess the thermal performance of a full-scale embedded energy wall to better understand its short-term behaviour under building climate control conditions.
d) Analyse temperature variation in the energy wall and surrounding soil during both intermittent and continuous thermal performance tests (TPTs).
e) Provide experimental data to support the design of energy walls in regions with climatic and geotechnical conditions similar to those of the study area.
f) Develop a numerical model of the same experimental set-up and validate it against the field results.

g) Additionally, use an analytical model for energy walls and test it against the experimental outputs, to see if the dual pipe arrangements can be tested through an analytical approach.

Finally, this study addresses a key research gap by investigating the intermittent operation of energy geostructures and their potential for ground recovery in Brazilian climate and soil conditions, representing the central novelty of this work. The findings offer valuable guidance for the design and operation of energy-efficient wall systems in regions with unsaturated soils and high cooling demand, providing practical insights for engineering applications.

2. Experimental program

2.1. Test site

Ten energy wall panels—serving as field prototypes of basement retaining walls for buildings—were constructed at the Test Site of the EESC-USP, located at the São Carlos School of Engineering, University of São Paulo (USP), in the city of São Carlos, São Paulo State. The site is characteristic of the unsaturated tropical soil conditions commonly encountered in Brazil. São Carlos experiences dry winters and wet summers, with the rainy season extending from November to April. In 2024, average daily temperatures ranged from 17.9 °C to 29.2 °C [18]. The soil profile at the test site, shown in Figure 2, consists of a residual sandstone layer—classified as medium- to fine-grained sand with variable clay content—overlain by a superficial layer of lateritic clayey sand (colluvial soil). These two layers are separated by a prominent bed of pebbles [19,20]. The upper layer has undergone intense tropical weathering, driven by high temperatures, heavy rainfall, and efficient drainage. As a result, it exhibits high porosity and remains unsaturated, with collapsible behaviour.

The groundwater table depth at the site fluctuates seasonally between approximately 9 and 12 meters below the ground surface, as shown in Figures 2 and 3. Figure 2 also presents the natural void ratio within the upper 9 meters of the soil profile, which ranges from 1.2 to 0.67 [19]. According to the chemical composition analysis conducted in [12], quartz is the predominant mineral throughout the soil profile. The high quartz content may contribute to increased thermal conductivity of the soil [24,25].

The seasonal variation of soil moisture content, as reported by various authors at the test site, reflects clear fluctuations driven by alternating dry and rainy periods. These variations significantly influence the seasonal changes in the soil's thermal conductivity. A similar effect was observed by [12] during thermal response tests conducted on an energy pile installed at the same location. Based on the measurements presented in this figure, the energy walls in the current study were constructed with an embedment length of 3.5 meters. Consequently, they were fully installed within the unsaturated soil zone and are subject to seasonal fluctuations in soil moisture content.

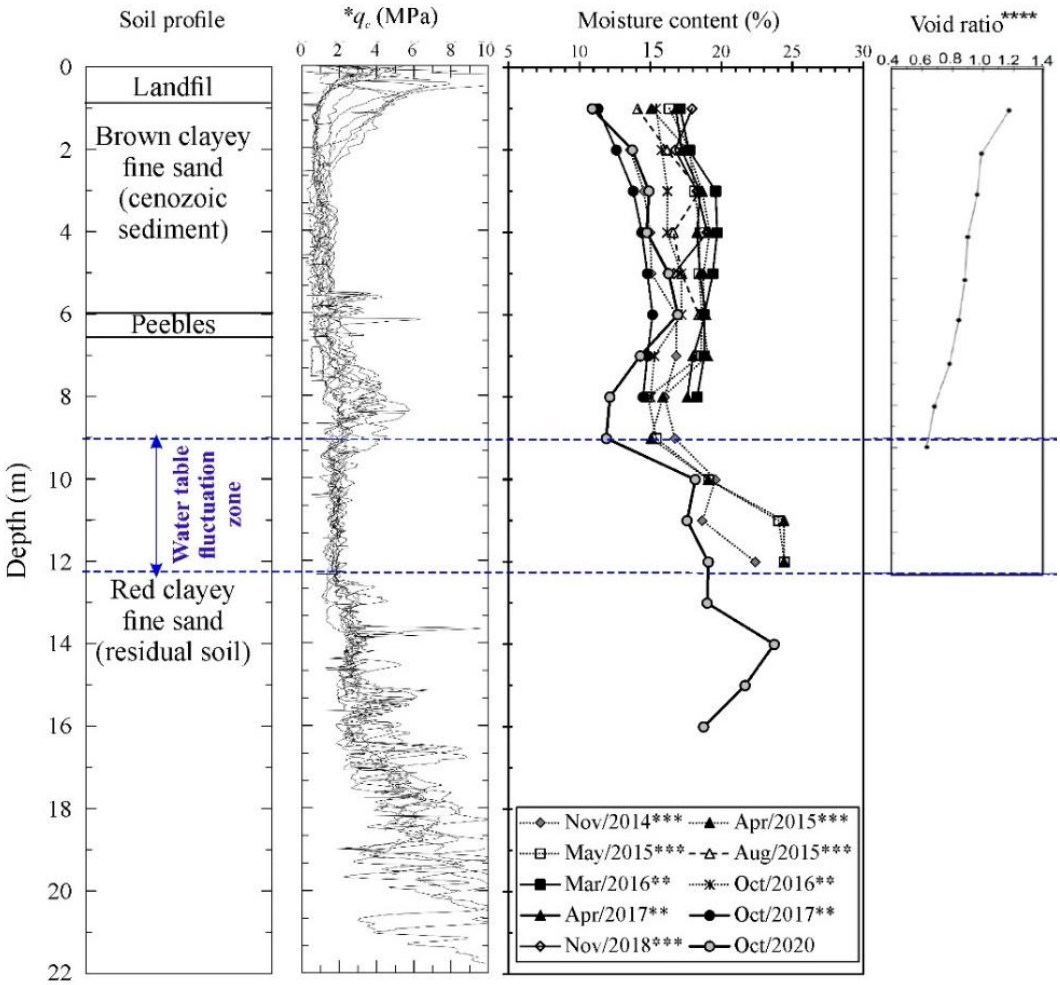

Figure 2. Soil characteristics of the test site obtained in previous studies (*[20], **[21,22], ***[12], ****[19]).

The distribution of gravimetric water content in unsaturated soils is closely linked to soil suction, which governs the thickness of water films surrounding soil particles and the formation of water bridges between them—factors that play a critical role in influencing soil heat flow and thermal conductivity [26]. In this study,

soil matric suction at the test site was monitored by [27] using Watermark Granular Matrix Sensors (GMS), installed at depths of 1.0 and 2.7 meters.

The highest average matric suction values were recorded in August and September 2024, reaching approximately 110 to 142 kPa at a depth of 1.0 m, and 73 to 112 kPa at 2.7 m. In contrast, the lowest values were observed in April 2023—at the end of the rainy season—measuring around 12.0 kPa at both depths. The results for matric suction, groundwater table depth, and monthly precipitation over a two-year monitoring period are presented in Figure 3. This figure illustrates a clear correlation between precipitation and matric suction within the topsoil layer (up to approximately 3 meters), where increased precipitation corresponds to reduced suction.

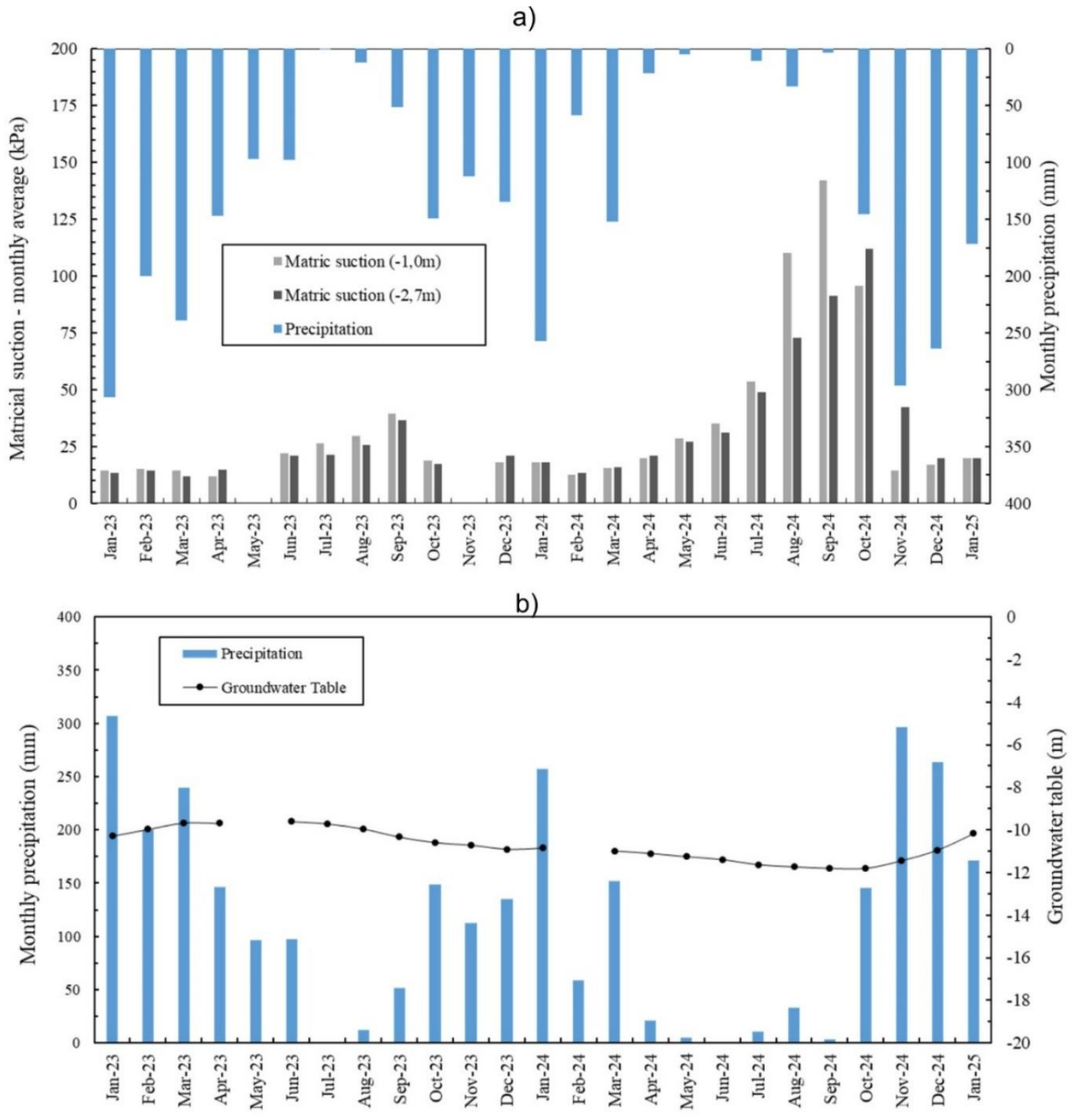

Figure 3. (a) Matric suction and monthly precipitation at the test site (precipitation data from [18], and suction data from [27]; (b) groundwater table depth and monthly precipitation at the test site [27].

In previous studies on the thermal behaviour of heat exchanger piles at the test site, temperature sensors were installed at depths of 3.5 m, 7.5 m, and 11.5 m. The natural ground temperature was monitored in 2015 and 2016 by [12,23], showing an average of approximately 24 °C, consistent with earlier observations by [20]. This value aligns with typical tropical subsoil temperatures, which generally range between 20 °C and 25 °C [9].

To characterize the soil's thermal conductivity, four distinct types of tests were previously performed at the site: thermal response tests (TRT´s) on a small-diameter energy pile (250 mm in diameter and 12 m in length) [12]; laboratory thermal needle probe tests on disturbed and remolded samples from the site [31]; thermal cone penetration tests (T-CPT) [30]; and thermal dynamic probing light tests (T-DPL) [29]. Table 1 summarizes the soil thermal conductivity (λ) values reported in previous studies for the upper 4 m of the test site, corresponding to the depth at which the energy walls of the current study are installed. Results from the thermal response tests (TRTs) are not included, as these tests were used to determine the average thermal conductivity of the upper 12 m layer, encompassing both unsaturated and saturated soils.

Table 1. Previous results of soil thermal conductivity (λ) obtained at a depth of 3.0 m at the test site.

Test type	Saturation degree (%)	λ (W/m °C))
Laboratory thermal needle probe (remolded sample) by [31]	48	1.16
T-DPL in April/2024 by [29]	50	2.13
T-DPL in July/2024 by [29]	40	1.37-1.52
T-CPT in April/2023 by [30]	50	1.42-1.67

As shown in Table 1, the thermal conductivity values obtained from the T-DPL tests conducted in April 2024 (end of the rainy season) were higher than those measured in July 2024 (mid-dry season), highlighting the influence of the degree of saturation on the thermal conductivity of unsaturated soils. Thermal conductivity values derived from T-CPT and T-DPL tests were higher than those obtained in laboratory needle probe

measurements [31] at comparable saturation degree. This difference can be explained by factors including in-situ stress conditions, sample disturbance, and the limited size of laboratory specimens [32].

2.2. Energy walls

The energy walls tested in this study consisted of two adjacent panels (numbered 4 and 5 in Figure 4) of a concrete energy wall. Each panel measured 3.5 m in length, 0.45 m in thickness, and 1.5 m in width. The walls were fitted with horizontally arranged high-density polyethylene (HDPE) pipes, having an outer diameter of 20 mm and an inner diameter of 15.4 mm (Figures 4c–e), with a spacing of 300 mm.

Figure 4. (a) Dimensions and locations of the energy wall panels; (b) Excavation process; (c) Installation of steel cage with HDPE pipes; (d) Steel cage with HDPE pipes prior to installation; (e) Temperature sensors embedded in the steel cage; (f) Wall panels 4 to 8 during concrete curing.

The excavation process is shown in Figure 4b, while the wall panels after concreting are shown in Figure 4f. Figure 4e shows the installation of Pt-100 Class A platinum thermistor sensors within the reinforced steel cages. These sensors, manufactured by Salcas Indústria e Comércio Ltda, have an accuracy of ±0.15°C at 0°C, ±0.35°C at 100°C, and operate over a range of 0–250°C. These sensors were used to monitor temperature

variations along the wall depth during the thermal performance tests (TPTs). A second group of Pt-100 sensors was embedded in the ground to monitor soil temperature. These were installed in two boreholes located 0.5 m and 1.0 m away from the tested energy walls (Panels 4 and 5). The sensors were placed at depths of 1.2 m, 2.2 m, and 3.2 m to capture temperature variations across the full vertical extent of the energy walls, as shown in Figure 5.

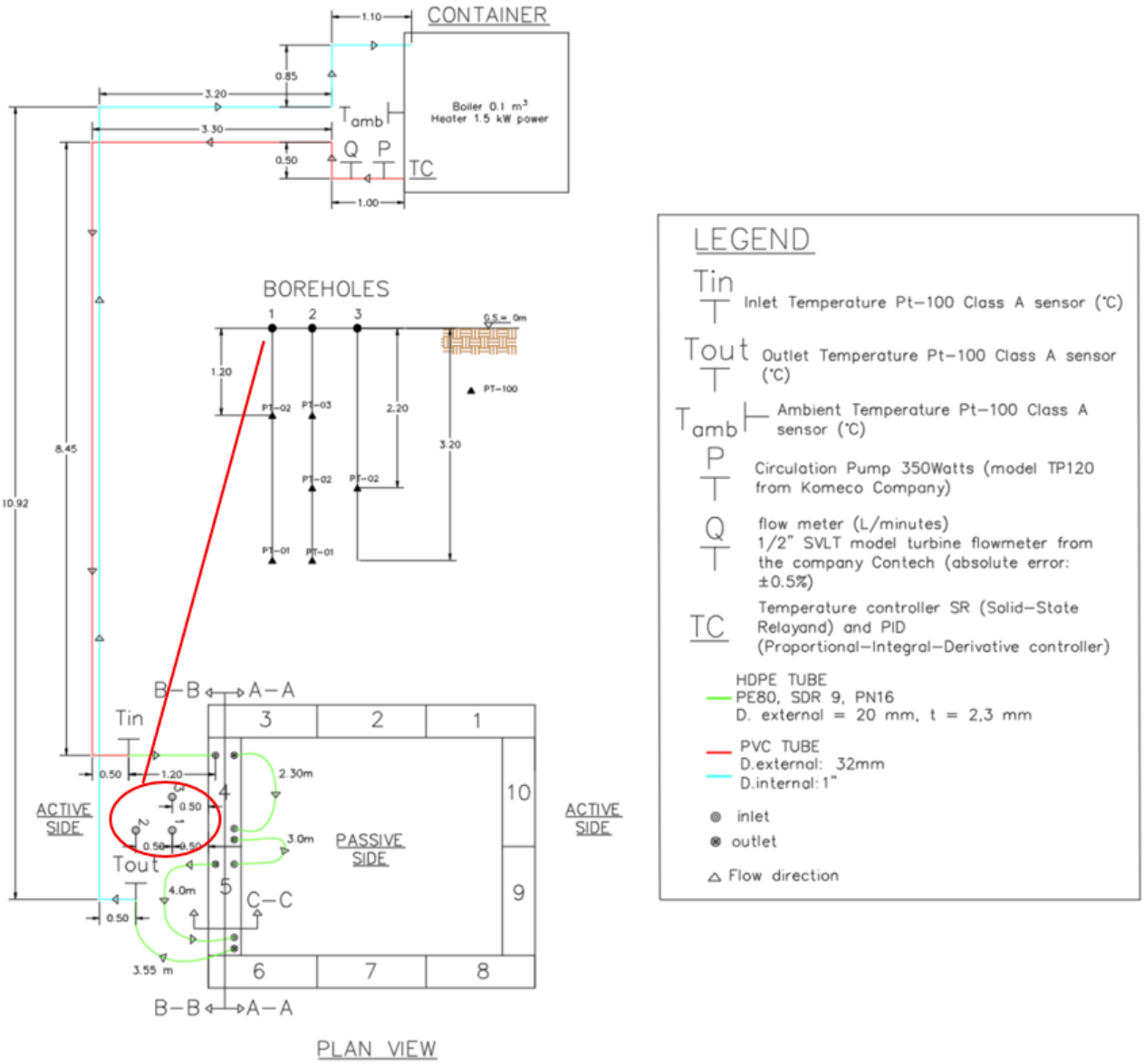

Figure 5. Schematic diagram of the energy wall testing configuration: (a) Water circulation circuit within the pipes and temperature instrumentation (Pt-100 sensors) embedded in energy wall panels 4 and 5; (b) Ground temperature monitoring boreholes. (Figures not to scale; dimensions are in meters)

The tests in the current study were designed to simulate the lower section of an energy retaining wall with soil on both sides, as illustrated in Figure 1. In a subsequent phase of this research—not covered in this article—the topsoil zone between the walls shown in Figure 4 will be excavated. This planned excavation is why Figure 5 indicates the passive and active sides of the walls. It will allow for testing of the retaining wall under the conditions illustrated in Figure 1, where the lower sections remain in contact with soil on both sides, while the upper section is exposed to soil on only one side.

2.3. Thermal performance tests

Two in situ Thermal Performance Tests (TPTs) were conducted in this study to assess the thermal behaviour of an energy wall section in contact with tropical unsaturated soil on both sides. The tests took place between December 2024 and January 2025, during the hot-humid season. During this period, increased precipitation led to a higher degree of soil saturation near the wall (Figure 3), coinciding with significantly elevated building cooling demands compared to the dry season. Throughout both tests, the soil remained in a consistently unsaturated condition typical of the rainy season. Consequently, the results from the two TPTs—one conducted under continuous operation and the other under intermittent operation—are directly comparable and provide valuable insights into system performance under peak cooling demand conditions.

The experimental setup for the TPTs conducted in this study is illustrated in Figure 6. The system comprises a 0.1 m^3 hot water reservoir, a circulation pump, a flowmeter, and two electric resistances installed within the reservoir, capable of delivering up to 1500 W of heating power. A temperature control system was implemented to maintain a constant inlet temperature. This system includes a Solid-State Relay (SSR), an electronic switching device, and a Proportional-Integral-Derivative (PID) controller, which minimizes control errors and maintains system stability. For heating temperature regulation, a Type J thermocouple (labeled “TC” in Figure 5) was installed inside a PVC tube, positioned just outside the hot water reservoir.

Temperature sensors and a data logger were integrated into the setup to monitor and record test data continuously. Three Pt-100 Class A thermistor sensors were used to measure the inlet (T_{in}) and outlet (T_{out}) temperatures of the heat exchanger loops embedded in the energy walls, as well as the ambient (external) air temperature (T_{amb}). All sensors, including those in the test setup, energy walls, and surrounding boreholes, were connected to a PMX data logger (Catman® software; multi-channel system, Hottinger Baldwin Messtechnik

GmbH – HBM) for continuous data acquisition. To minimize heat losses to the environment, the entire piping system was insulated using glass wool, elastomeric foam, and aluminized adhesive tape.

For this investigation, two short-term in situ Thermal Performance Tests (TPTs) were conducted to assess the heat exchange efficiency of the energy wall and to compare the performance of a ground source heat pump (GSHP) system operating under intermittent and continuous modes in tropical unsaturated soil conditions. The tests were carried out between December 2024 and January 2025, aligning with São Carlos's hot-humid season. During this period, the surrounding soil layer exhibits a higher degree of saturation due to increased precipitation, and building cooling demand is significantly higher compared to the dry season.

Figure 6. Experimental setup of the TPT's conducted in this study.

During the tests, the inlet temperature and flow rate of the circulating fluid (water) were kept constant. The outlet temperature and flow rate were recorded simultaneously to calculate the heat exchange per unit area of the energy wall surface in contact with the soil, as given by Equation 1:

$$q = \frac{c \cdot \dot{m} \cdot (T_{in} - T_{out})}{A} \quad (1)$$

Where q is the heat exchange amount per unit area of the energy wall (W/m^2); c is the specific heat of the circulating fluid (J/kg◦C); $\dot{m}$ is the mass flux of the circulating fluid (kg/s); T_{in} and T_{out} are the fluid inlet and outlet temperatures (◦C); A is the active area of the energy wall (m^2).

During the heating phase of the tests, the inlet temperature was maintained at 35 °C to simulate building cooling operation conditions, and flow rate of the circulating fluid ranged from 9.5 to 10.5 L/min, ensuring fully turbulent flow within the heat exchanger pipes. According to Choi et al. [33], the typical duration of a Thermal Performance Test (TPT) on energy piles is approximately 100 hours. In this study, two TPTs were carried out: a continuous test lasting ~96 hours (~4 days), and an intermittent test with 12-hour heating cycles, also over ~4 days. Reflecting the typical 12-hour daily operation of air-conditioning in commercial and institutional buildings in Brazil, the intermittent TPTs in this study employed 12-hour pauses. However, future works should investigate the impact of different pause durations. Details of the tests are provided in Table 2. The test durations ranged from approximately 4 days, aligning with durations adopted in similar studies for comparison purposes [6, 28].

Table 2. Duration of the two TPT's conducted on the heat exchanger wall (panel 4 + panel 5).

TPT type	Begin of the heating test	End of the heating test	Number of cycles	TPT duration (h)	Recovery time after TPT (h)
Continuous	11:09 a.m. December 20th 2024	12:00 a.m. December 24th 2024	-	96	475
Intermittent	5:02 p.m. January 18th 2025	6:50 p.m. January 22th 2025	4	97	-

In the TPT simulating continuous operation of a GSHP system, both the circulation pump and the heater remained active 24 hours a day, resulting in uninterrupted heat injection into the ground. In contrast, under

intermittent operation, the pump and heater were activated for 12 hours per day, followed by a 12-hour shutdown. This alternating cycle allowed partial recovery of the soil and wall temperatures between heating periods. Continuous operation typically results in heat accumulation around the energy wall, which can gradually reduce system performance over time. Conversely, the cooling intervals in intermittent operation help moderate temperature increases, potentially enhancing overall thermal efficiency. A similar trend was reported by Hu et al. [34], who observed a slightly lower average heat transfer flux under continuous operation (83.68 W/m²) compared to intermittent operation (92.22 W/m²) during a thermal response test conducted at 3 kW on an energy wall.

3. Numerical and analytical models

Table 3 presents a summary of the material properties utilized in the numerical and analytical models developed in the present study.

Table 3. Material properties used in the numerical and analytical models.

Property	Model	Value	Source
Soil			
Thermal Conductivity	Numerical	2.13 W/mK (0-4.5m) 2.10 W/mK (4.5-6.5m)	[29]
	Analytical	2.13 W/mK	
Density	Numerical	16.52 kN/m³ (0-4.5m) 16.8 kN/m³ (4.5-6.5m)	[12]
	Analytical	16.52 kN/m³	
Heat Capacity	Numerical	800 J/kgK	[29]
	Analytical		
Wall (RCC/Concrete)			
Thermal Conductivity	Analytical and Numerical	2.3 W/mK	[35]
Density		2,400 kg/m³	
Heat Capacity		880 J/kgK	
Heat exchanger pipe			
Thermal Conductivity	Analytical and Numerical	44.5 W/mK	[10]
Density		8060 kg/m^3	
Heat Capacity		400 J/kgK	
Circulating fluid - Water			
Thermal Conductivity	Analytical and Numerical	0.59 W/mK	[41]
Density		1000 kg/m^3	
Heat Capacity		4226 J/kgK	

3.1. Numerical Models – COMSOL Multiphysics

A full-scale three-dimensional numerical model has been developed in COMSOL Multiphysics [36] – version 6.1 – to validate it against the experimental results from the site. These are finite element numerical models developed in the form of individual panels and then assembled in the application. Prior to assembly, in panels 4 and 5, embedded pipes are modelled using 2D line elements. In other panels, these pipes are not installed as those panels are not thermally activated – as discussed before. Once assembled, the pipes of panels 4 and 5 are connected to each other via line elements by introducing additional planes in the numerical model. These can be seen in Figure 7. In the numerical model, the soil is assembled around and inside the wall in the form of layers to address.

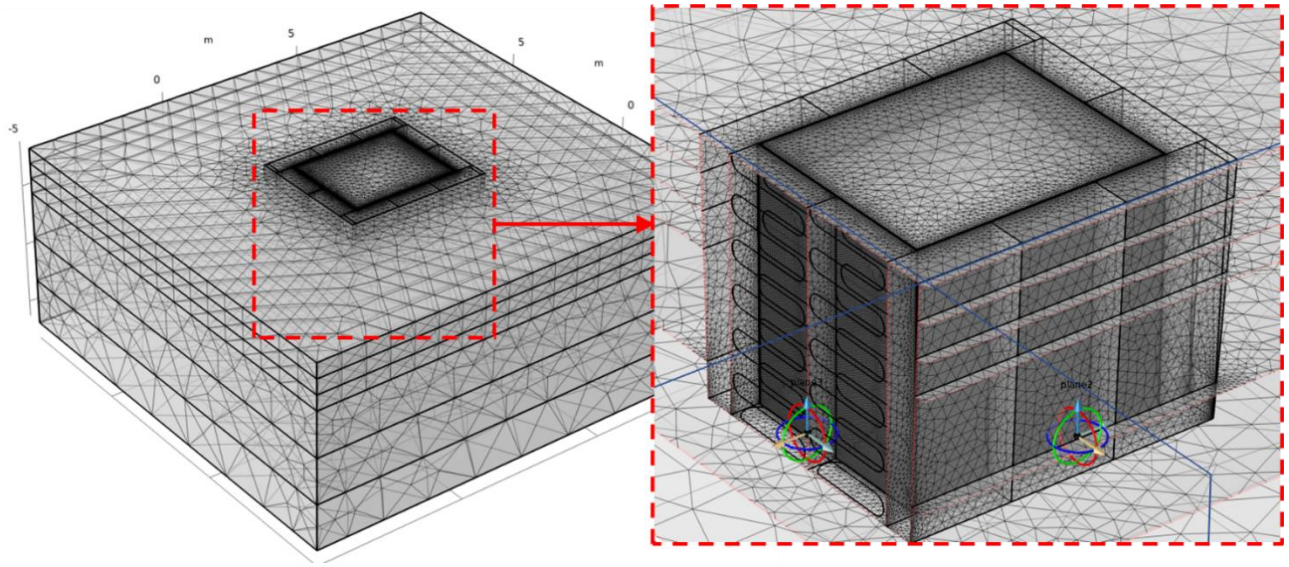

Figure 7. Finite element numerical models that were simulated for validation, along with the mesh.

The numerical models are applied with a custom mesh setting in which the mesh size starts from 0.01m, with a growth rate of 1.3, which makes it have much smaller sizes inside and near the energy wall itself, while keeping the highest size of 2m for the region much further away from the soil. This gives around 2,676,388 domain elements, 260806 boundary elements, and 9192 edge elements. This assists in keeping calculations accurate near the necessary region through fine meshing, while keeping the run time low through coarse meshing. The top surface of the numerical model is applied with the ambient temperature extracted from the experimental setup, while the bottom face and side faces are applied with Far-Field Temperature (FFT). The ground length has been extended sufficiently to ensure that temperature effects at the far end do not influence the result extracted through the models. The initial temperature of the numerical models was applied based on

depth. These temperatures were taken from the initial readings of Pt-100 sensors that were installed in the soil at 1.2m, 2.2m and 3.2m. These depth-based temperatures were also used as FFT on the side surfaces of numerical models. The study uses data from both continuous and intermittent testing to validate the numerical models.

3.2. Analytical Models – FIS Method

There are only a few studies which discuss analytical methods for thermal analysis of the energy walls [11,37,38,39]. Out of these, the Flux and IPS Splitting (FIS) method [37] is adopted for this study. This method assumes the formation of a heat plane due to repetitive arrangements of the embedded heat exchanger pipes. These heat planes are equated to Infinite Plane Sources (IPS), which are the infinitely large planes that are used as heat sources or sinks. The concept of infinitely large planes as heat sources was first introduced by Carslaw & Jaeger [40]. Using IPS as base models, the FIS method can be used for thermal analysis in this case as well.

For using the FIS method, the three-dimensional model first needs to be simplified into its simplest form, which here can be simplified to a rectangular cross-section representing the wall, with two pipes from the repetitive pattern along the height of the wall, as can be observed in Figure 8.

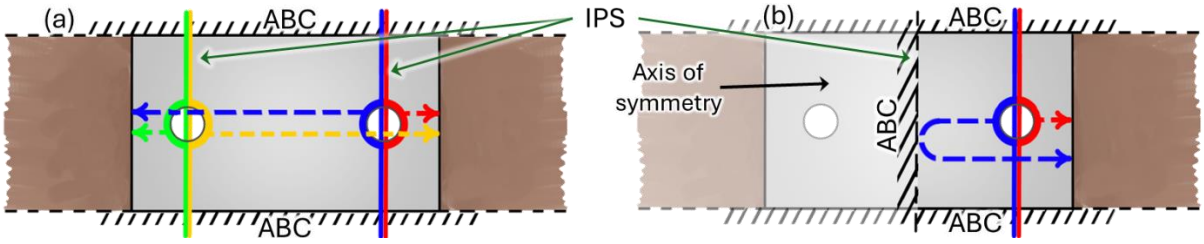

Figure 8. Schematic representation of (a) cross-sectional geometry of the repetitive pipe arrangement within the wall with placement of the Infinite Plane Source (IPS) and (b) simplified geometry using symmetry with Adiabatic Boundary Condition (ABC)

Based on the cross-sectional geometry shown in Figure 8, the FIS methods can be applied in two ways. In the first method, it can be achieved by applying two planes on each pipe and using the heat transfer in each direction to calculate the temperature changes on either surface, thereby using four IPS planes in total, as shown in Figure 8a. On the other hand, in the second method, the symmetry of the cross-section can be used. In this, the Adiabatic Boundary Condition (ABC) is applied to the line of symmetry, and the resulting geometry (as

shown in Figure 2b) can be treated as the Energy Wall with exaction side, or the GE case from [37]. This method only uses two IPS planes to perform thermal analysis of the energy walls. Therefore, a general solution for calculating the average temperature change in the fluid (ΔT_{avg}) over the pipe network can be given by Equation 2.

$$\Delta T_{avg} = \frac{q_p}{N\lambda} G(x_\omega, t) + q_\omega s(R_W) + q_p s(R_P + R_f) \quad (2)$$

Here N=4, as it is the number of IPS planes. q_p represents the planar heat flux (W/m^2). G(xω,t) – G-function for IPS – calculates temperature changes at any time t, at the distance of x_ω, and pipe spacing is represented by s. Thermal resistivity for wall, pipes and fluid are represented by R_W, R_P and R_f, respectively. The equations of R_P and Rf are well established and are extracted from [41]. Whereas for G-functions, the simplified equation for this case is given by [42] and mentioned in Equation 3.

$$\frac{q_p}{N\lambda_g} G(x_\omega, t) = \sum_{i=1}^{n} \left(\frac{q_{p_i} - q_{p_{i-1}}}{4\lambda_g}\right) \left(\sqrt{\frac{4\alpha_g (t_n - t_{i-1})}{\pi}} \left(e^{-{x_1}^2 . (t_n - t_{i-1})^{-1}} + e^{-{x_1}^2 . (t_n - t_{i-1})^{-1}} \right) - x_1 \, erfc \frac{x_1}{\sqrt{4\alpha_g (t_n - t_{i-1})}} - x_2 \, erfc \frac{x_2}{\sqrt{4\alpha_g (t_n - t_{i-1})}} \right) \quad (3)$$

Where, x_1=c+0.5D, which is the distance of the first IPS which transfers heat directly with the closest ground surface, whereas, x_2= W-x_1, which is the plane which faces towards the line of symmetry, and the heat transfer bounces from that surface and exits from the same ground-wall interface, as shown in Figure 8b. The time step at which the temperature changes are calculated is represented by n. Thermal conductivity and diffusivity of the ground are given by λ_g and α_g, respectively. D and c are pipe diameter and pipe cover, respectively. Also, erfc is the complementary error function. As for the thermal resistance of the wall, R_W, it is estimated using shape factors (S_F) as given by [37] and mentioned in Equation 4.

$$S_F = \frac{2\pi}{\ln\left(\frac{2s}{\pi D} sinh\left(\frac{2\pi(c+0.5D)}{s}\right)\right)}; \quad \text{also, } R_W = \frac{1}{\lambda_W S_F} \tag{4}$$

The thermal conductivity of the wall is represented by λ_W. Therefore, Equations 3 and 4 are incorporated into Equation 2 to determine the variations in output fluid temperature of the energy wall. This analytical method is used for predicting outlet fluid temperature for both continuous and intermittent tests.

4. Results and discussions

4.1. TPT results

The results of the two Thermal Performance Tests (TPTs) conducted on wall panels 4 and 5—connected as a single panel—are presented in Figure 9, covering both intermittent and continuous operation modes. A fundamental aspect of TPTs is maintaining a nearly constant inlet temperature of the heat transfer fluid (approximately 35 °C in this study). As the fluid circulates through the heat exchanger at a specified flow rate, heat is transferred to the surrounding soil, leading to a measurable temperature difference between the inlet and outlet. Throughout the tests, both inlet and outlet fluid temperatures were continuously recorded. Additionally, the water circulation flow rate (constant = 10 L/min) and ambient air temperature were monitored. Figure 9 also shows these initial operating parameters for both TPTs on the energy wall.

The continuous TPTs conducted in the hot season show a minimal effect of ambient air temperature (T_{amb}) on inlet (T_{in}) and outlet (T_{out}) fluid temperatures, even though the external PVC pipes were thermally insulated with stone wool, elastomeric material, and aluminized tape (Figure 6). During the continuous heating test, the inlet temperature began to exceed 35 °C between 30 and 45 hours into the experiment (Figure 9a). To maintain the inlet temperature near the target value of 35 °C, the temperature control system was adjusted to activate the heater whenever the thermocouple registered a temperature within the range of 35 ± 3 °C. This adjustment, implemented at hour 49 of the test, successfully stabilized the inlet temperature around 35 °C for the remainder of the experiment.

During intermittent operation (Figure 9b), noticeable temperature peaks occur at the beginning of each cycle. When the system restarts, a transient period is required for the hot water supplied by the reservoir to

equilibrate with the water already present in the energy wall pipes. Consequently, the inlet and outlet temperature sensors take some time to stabilize.

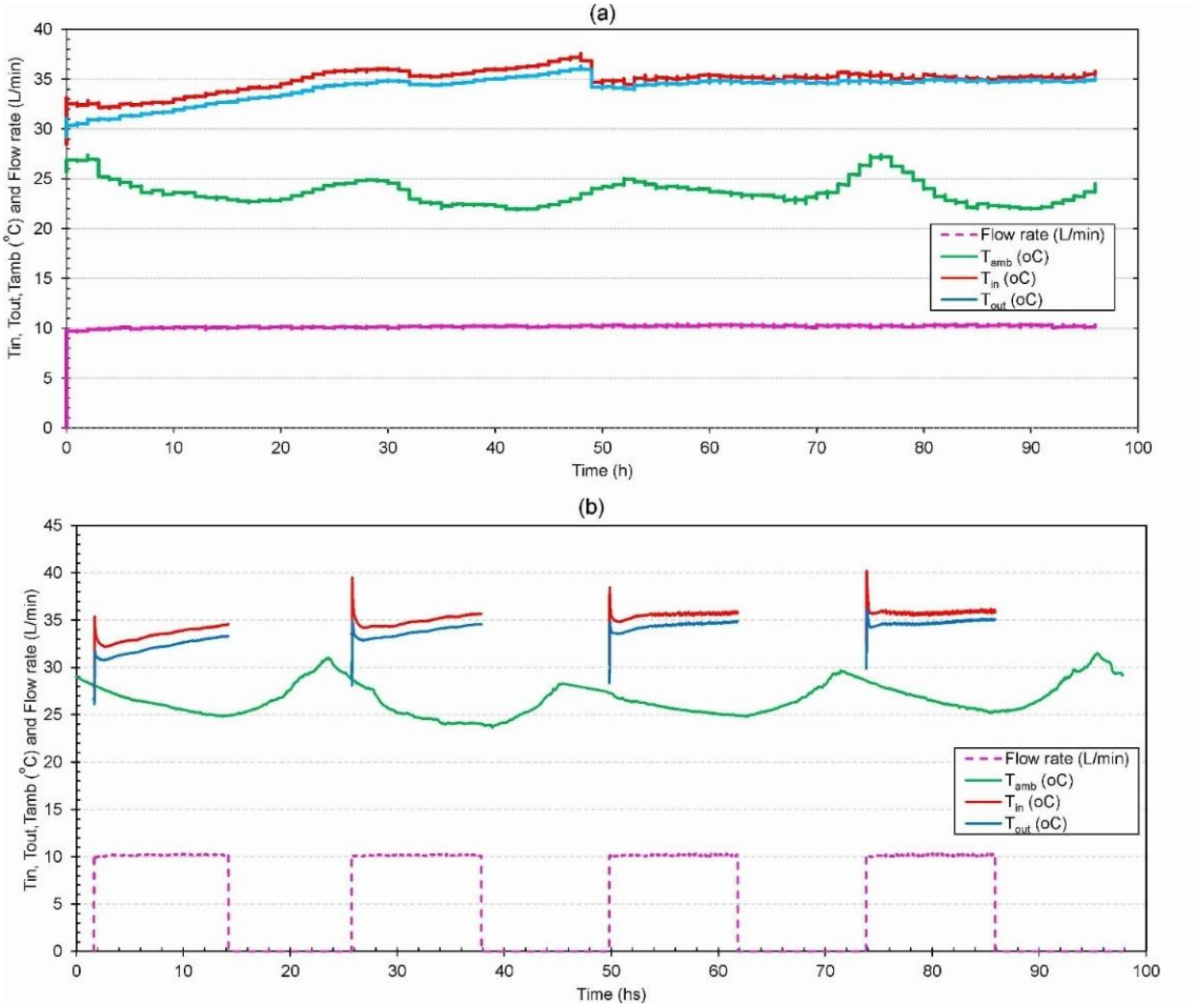

Figure 9. Results of of T_{amb}, T_{in} and T_{out} temperatures, and flow rate during the two TPT tests: (a) continuous mode: (b) intermittent mode.

4.2. Temperature in the wall panels and in the surrounding soil

The results of temperature variation within the wall along its depth, as well as in the surrounding ground boreholes during the tests, are presented in Figures 10 to 16. Figures 10 and 11 show a comparison of temperatures recorded at corresponding depths by the Pt-100 sensors installed in the energy walls (panels 4 and 5). All depth sensors from the continuous heating test, along with the sensors up to 1.2 m deep in panel 5 during the intermittent test, recorded higher temperatures on the active side of panel 4 compared to both the active and passive sides of panel 5 (active and passive sides indicated in Figure 5). This pattern aligns with the hot water

flow direction within the wall system: as illustrated in Figure 5, hot water enters the system through the HDPE pipes installed on the active side of panel 4.

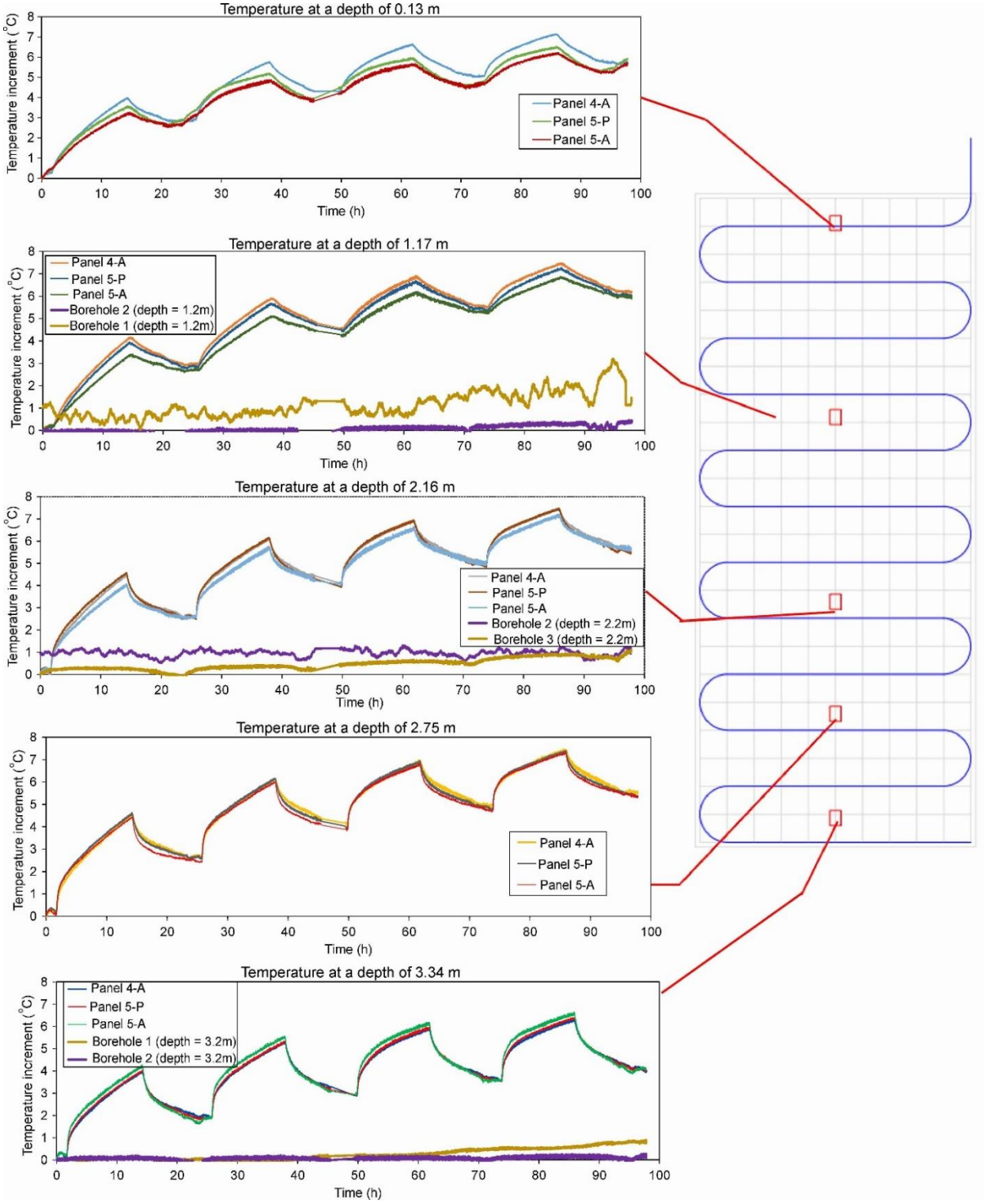

Figure 10. Intermittent mode test: temperature variation at different depths within the energy wall panels 4 and 5 and in the surrounding soil, where "A" is active side and "P" is passive side of the wall (Figure 5).

However, during the intermittent test, the sensors on the passive side of panel 5 at depths of 2.16, 2.75, and 3.34 meters recorded slightly higher temperature increases compared to those on the active side of panel 4. This behaviour is attributed to the intermittent nature of the test, which allows the system to partially recover its initial thermal state during the 12-hour pause periods. Since the soil temperature below approximately 2.5–3 meters remains relatively stable and is not significantly influenced by atmospheric conditions (typically around 24 °C), injecting water at 35 °C leads to more pronounced temperature increases at these deeper levels than at shallower depths (e.g., 0.13 and 1.17 meters), where temperature fluctuations are more strongly influenced by ambient conditions and heat dissipation.

On the other hand, the deep sensors (at 2.16, 2.75, and 3.34 meters) on panel 5 initially recorded higher temperature increases at the beginning of the continuous TPT compared to those on the active side of panel 4. However, as continuous heat injection progressed, the system began to stabilize after approximately 30 hours. From that point onward, panel 4 exhibited greater temperature variation than panel 5. This behaviour is consistent with the hot water flow path within the system, as the heated fluid enters through the HDPE pipes on the active side of panel 4 and gradually transfers heat to the surrounding soil.

The flow of hot water is also evident from the temperature readings of sensors installed on opposite sides of panel 5. Notably, the temperatures recorded on the passive side are consistently higher than those on the active side. This trend aligns with the internal flow path of the system, as illustrated in Figure 5: hot water exits panel 4 and enters panel 5 through the primary HDPE pipe circuit installed on the passive side.

During the continuous test, the sensor installed at a depth of 0.13 m recorded significant temperature fluctuations over time, primarily due to the influence of ambient air temperature. This oscillatory behaviour was not observed in the intermittent test, as the 12-hour heat injection pauses occurred during daytime hours (from 6 a.m. to 6 p.m.), when ambient conditions were more stable. While sensors installed at greater depths were also affected by ambient temperature variations, the impact was notably smaller—particularly after 175 hours from the start of the test, during the system's thermal recovery phase.

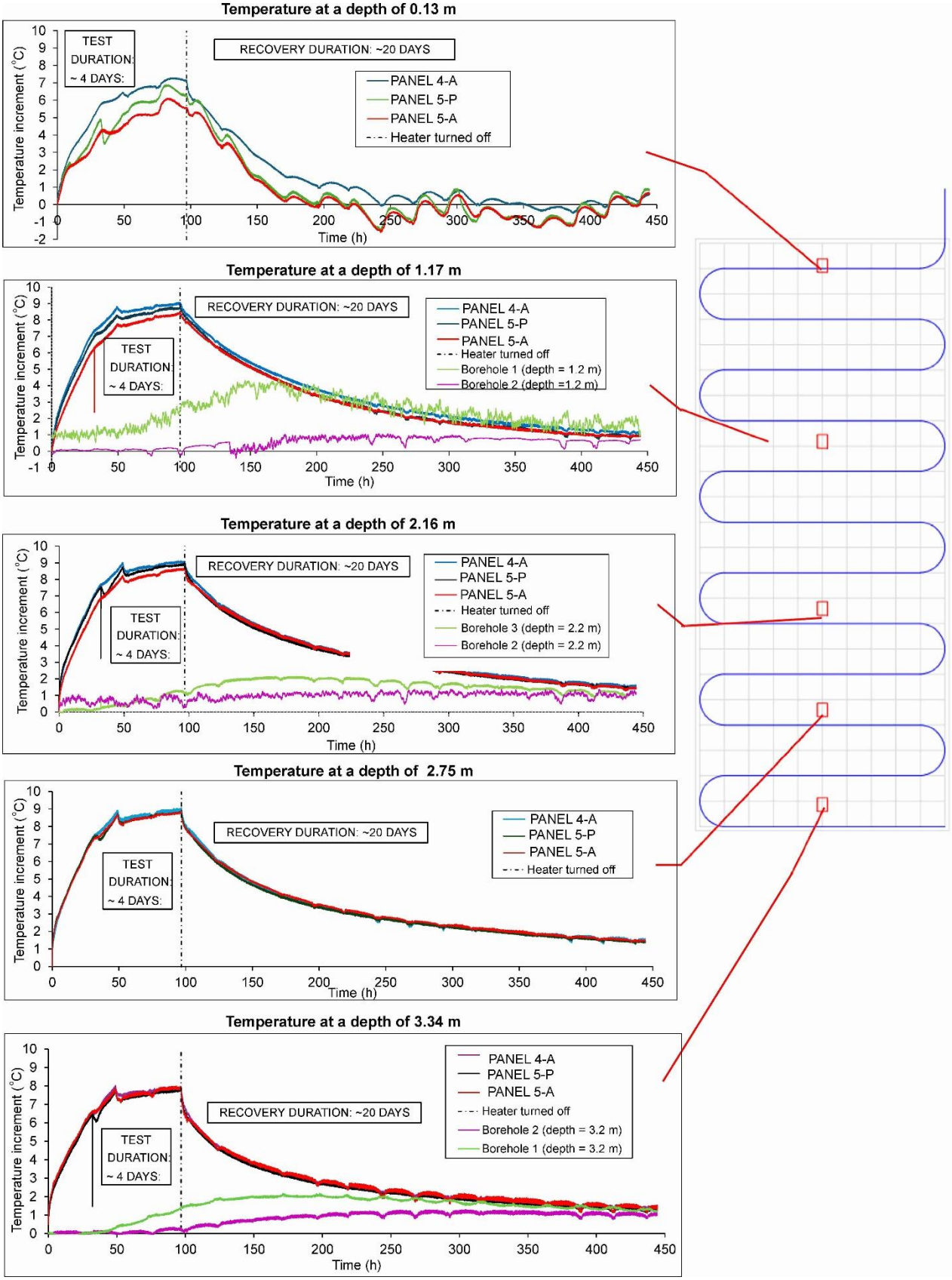

Figure 11. Continuous mode: temperature variation at different depths, depths within the energy wall panels 4 and 5 and in the surrounding soil, where "A" is active side and "P" is passive side of the wall during heating and recovery phases.

The adjustment made to the temperature controller to maintain the inlet temperature at approximately 35 °C is clearly noticeable around the 50-hour mark of the test. After 50 hours of continuous heat injection, the temperature within the wall began to increase at a significantly slower rate compared to the initial 0–50 hours. This change indicates the onset of thermal saturation in the surrounding soil, which led to a decline in the system's efficiency for cooling operations. This trend is supported by the sharp temperature rise observed in the borehole located 0.5 m from the wall, where the soil temperature increased by approximately 1 °C every 5 hours after the 50-hour point. This rate of increase continued until around 125 hours—roughly 25 hours after the heater and pump were turned off. In contrast, the borehole located 1.0 m from the wall showed a delayed response, with temperature increases beginning only after 100 hours of testing, coinciding with the shutdown of the heating system. However, the temperature rise in this borehole occurred at about half the rate observed at the 0.5 m borehole (approximately 0.5 °C every 5 hours) and stabilized by 150 hours.

A similar process of heat saturation in the soil was observed during the intermittent test (Figure 10), although it occurred with lower intensity and a delayed onset compared to the continuous test. At a depth of 3.34 m, the soil located 0.5 m from the wall began to show a temperature increase around 60 hours into the test—at the end of the third heating cycle—with a steady rise of approximately 0.1 °C every 5 hours. This rate represents only 20% of the temperature increase recorded at the same location during the continuous heat injection test.

At a depth of 2.2 m, a similar trend was observed, with a heating rate of about 0.15 °C every 5 hours, beginning at the same 60-hour mark. The sensor at 1.17 m depth recorded a slightly higher rate of 0.2 °C every 5 hours. This decreasing trend in temperature rise with depth can be attributed to increased thermal conductivity in the deeper soil layers. Enhanced heat conduction at greater depths reduces localized heat accumulation near the wall and, in turn, improves the system's efficiency in transferring heat to the ground. By the end of the 96-hour intermittent test, the soil at a distance of 1.0 m from the wall had not shown any significant temperature increase compared to the initial condition, further illustrating the slower and more distributed heat transfer process under intermittent operation.

Figures 12 and 13 illustrate the temperature increments measured on the external surfaces of the energy walls (reinforcement cages) at the locations of the installed Pt-100 sensors. During the 96 hours of the intermittent test, Figure shows smaller temperature increases at a depth of 3.34 m compared to the sensors

located near the surface, and a greater temperature increase at 3.34 m depth than at 0.13 m, which can be explained by the experimental setup: on the active side of wall 5, the hot water enters at the bottom and flows upward through the horizontal loops to the surface. Moreover, during the last heating cycle (fourth cycle, at around 75 hours into the test), the temperature increase over time was higher for the 0.13 m depth sensor compared to the 3.34 m depth sensor, as the temperature difference between the shallowest and deepest sensors decreased throughout the test. This observed behaviour is likely due to the reduced thermal conductivity of the upper soil layers combined with the 3.34 m depth sensor being located near the bottom of the wall.

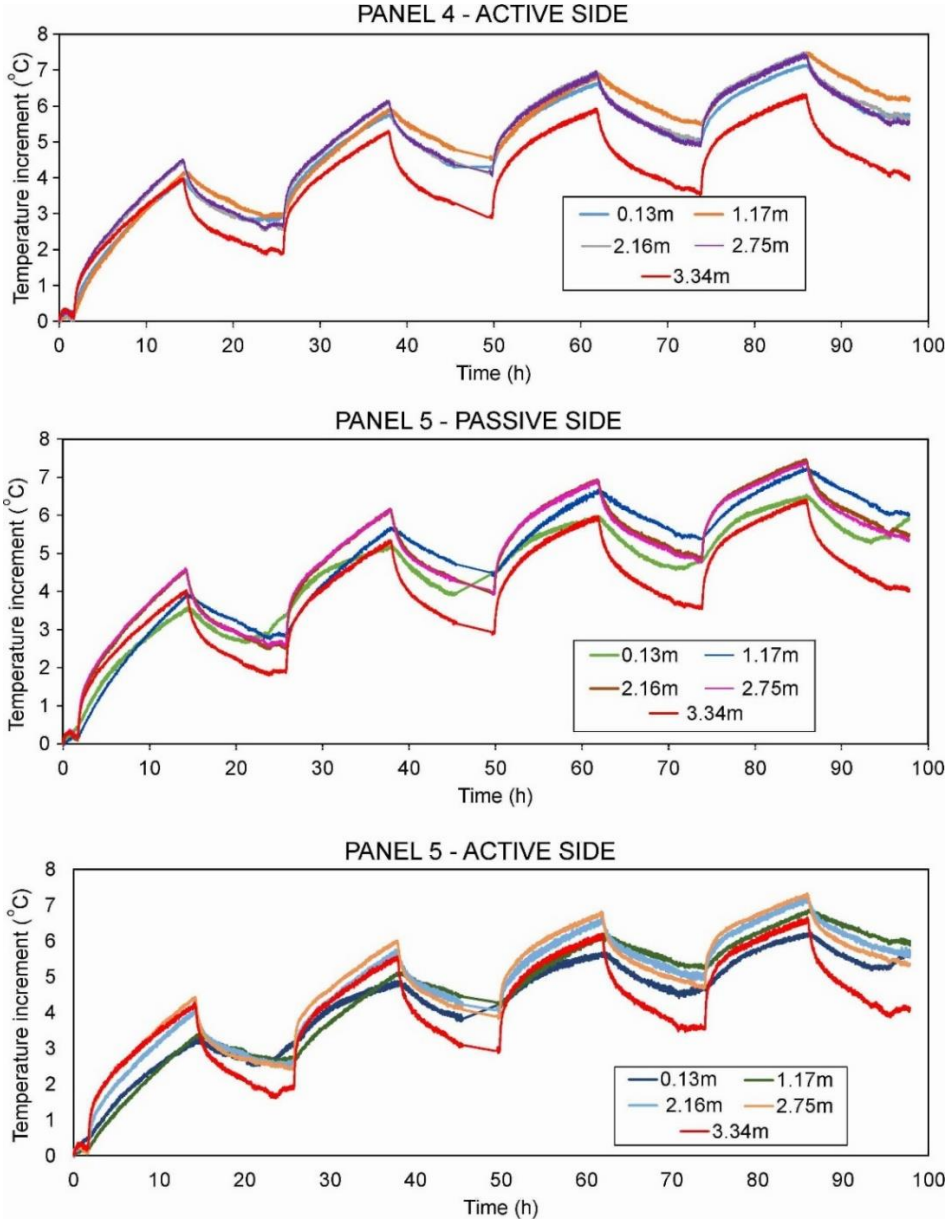

Figure 12. Intermittent mode test: temperature variation along the depth of wall panels 4 and 5, measured by PT-100 sensors installed in the reinforcement cage.

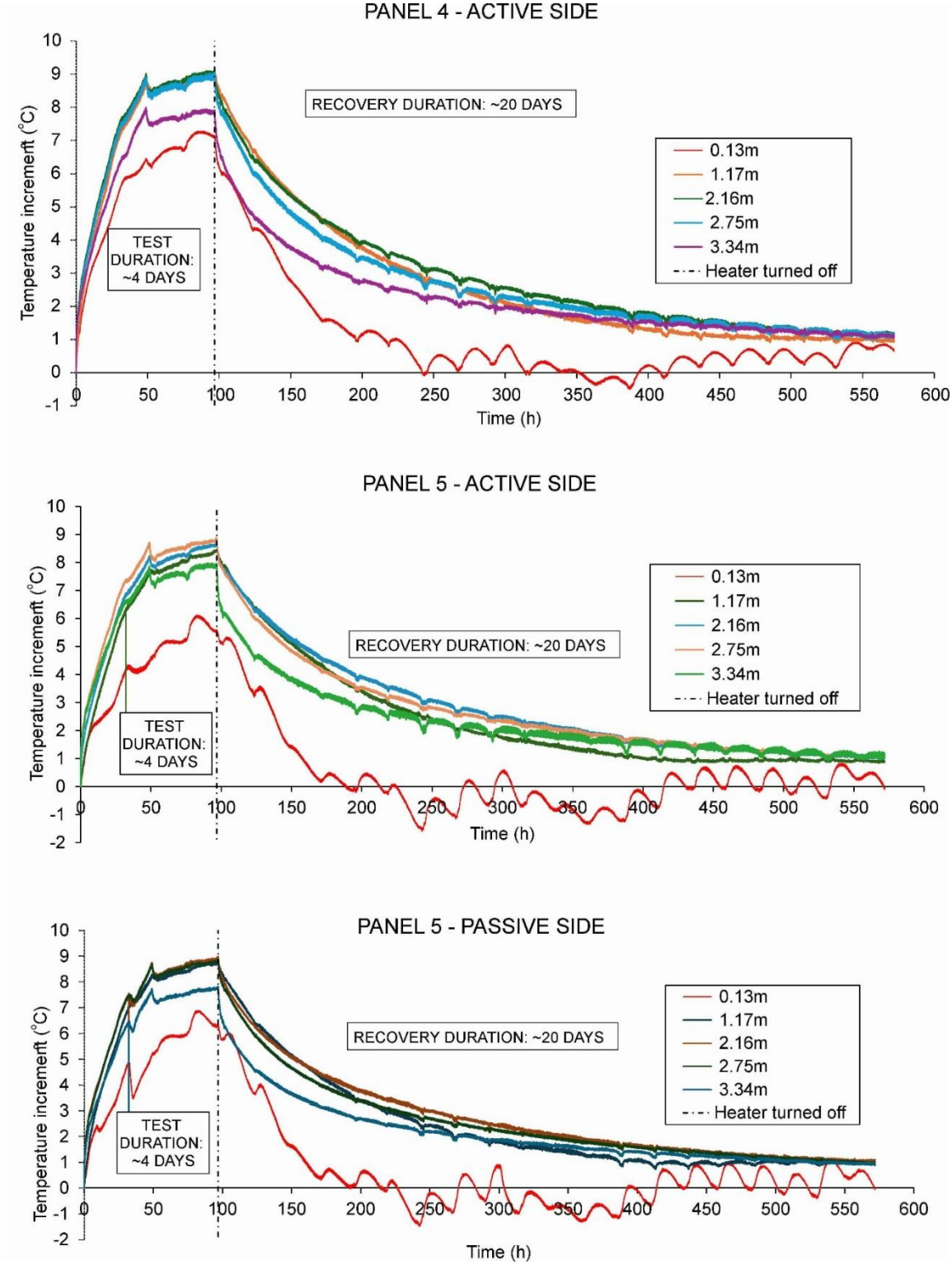

Figure 13. Continuous mode test: Temperature variation at each depth on the surface of each energy wall, measured by PT-100 sensors installed in the reinforcement cage, during heating and recovery stages.

Temperature variations along the wall depth were analysed at different moments during the continuous and intermittent tests conducted on embedded walls 4 and 5. The selected time intervals were based on two

specific criteria: (a) to span the entire test duration of 96 hours, from start to finish, and (b) to include only the periods when the system was 'on' during the four cycles of intermittent test. Accordingly, temperature increases were analysed at 0 h, 10 h, 34 h, 58 h, and 82 h. Figures 14 and 15 illustrate the results for the energy walls operating under intermittent and continuous modes, respectively.

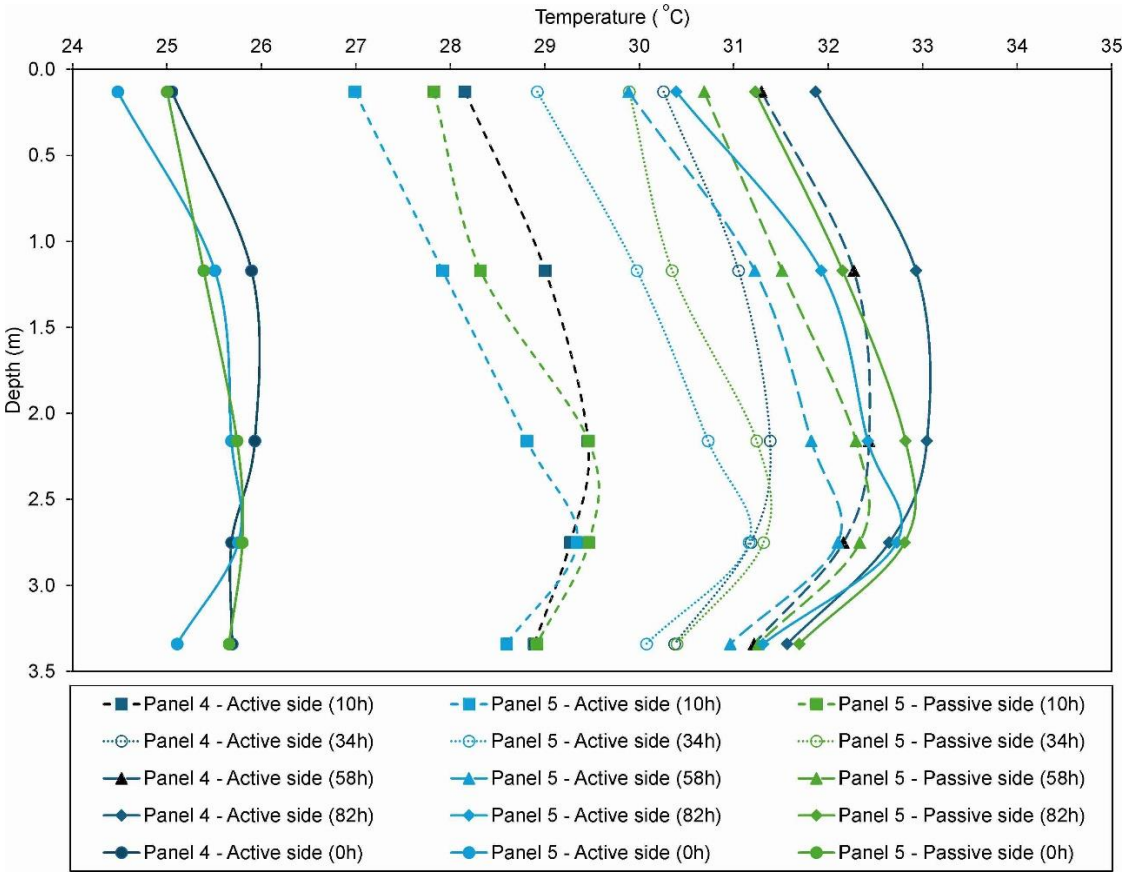

Figure 14. Temperature variation along the depth at different test intervals - 0 h, 10 h, 34 h, 58 h, and 82 h. – for the intermittent operation mode test.

In both heat exchange operation modes, a significant temperature increase is observed during the first 10 hours and again between 10 and 34 hours—particularly in the continuous test. After 34 hours, however, the rate of temperature rise begins to stabilize, likely due to the progressive warming of the surrounding soil, which reduces the thermal gradient between the circulating fluid and the soil. Additionally, the continuous test appears to reach thermal saturation around 58 hours, as no notable temperature increase is observed between 58 and 82 hours. By the end of the 82-hour continuous test, the wall temperature was approximately 1 °C higher than in the intermittent test.

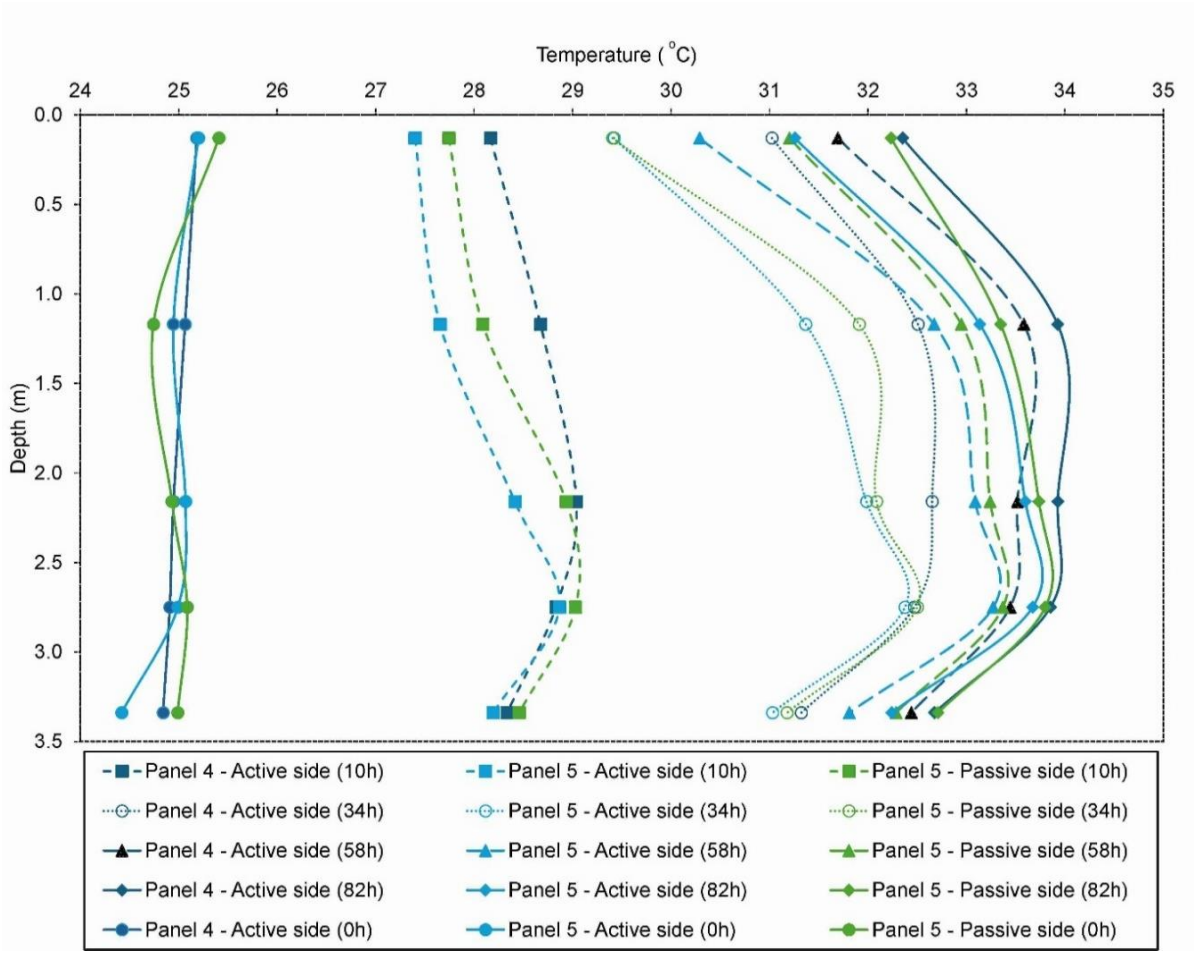

Figure 15. Temperature variation along the depth at different test intervals - 0 h, 10 h, 34 h, 58 h, and 82 h. – for the continuous operation mode test.

Along the wall depth, temperature variation was notably greater in the continuous test compared to the intermittent one. At 34 hours into the test, wall temperatures under continuous heating ranged from 29 °C to nearly 32.5 °C—an increase of approximately 3.5 °C (Figure 15). In contrast, during the intermittent heating test, temperatures ranged from 29 °C to around 31 °C, resulting in a smaller variation of about 2 °C. Moreover, beyond a depth of 2.5 meters, the temperature variation over time becomes smaller in both heating operation modes.

Figures 14 and 15 illustrate the heat transfer path through the exchanger pipes embedded within the energy walls. Hot water first enters the active and passive sides of panel 4, then flows to the passive side of panel 5 via the main pipe circuit and finally completes the loop on the active side of panel 5. Over time, the temperature along the wall depth is highest on the active side of panel 4, followed by the passive side of panel 5, and lowest on the active side of panel 5.

The continuous test was conducted from December 20 to 24, 2024, while the intermittent test began on January 18, 2025. At the start of the continuous test (0 h), the wall exhibited a nearly uniform temperature profile along its depth, averaging around 25 °C, with slightly higher temperatures (above 25.5 °C) near the surface—consistent with the thermal profile reported by [23] for the test site. In contrast, the intermittent test began with a temperature gradient ranging from 25 °C near the surface to 26 °C at a depth of 2.5 m. This suggests that the soil had not fully returned to its natural thermal state, even 25 days after four consecutive days of heating.

Figure 16 presents the variation in soil temperature surrounding the energy walls, as recorded by Pt-100 sensors installed in boreholes located 0.5 m (boreholes 1 and 3) and 1.0 m (borehole 2) from the walls, at depths of 1.2 m, 2.2 m, and 3.2 m. As shown in Figures 16a-b, during the heat injection phases of both TPTs (intermittent and continuous modes), temperature variations over time were more pronounced in the sensors located 0.5 m from the wall. In contrast, the sensors positioned 1.0 m away maintained relatively stable temperatures throughout the test.

The temperature increase in the soil was more pronounced during the continuous operation test, particularly between 50 and 96 hours, compared to the same period of the intermittent test with 12-hour heating cycles. For the sensor located 0.5 m from the wall at a depth of 1.2 m, a temperature rise of 1.5 °C was recorded during the final 30 hours of testing (Figure 16b). A similar trend was observed at depths of 2.2 m and 3.2 m at the same distance from the wall, although the temperature increase during the last 30 hours of continuous heating was approximately 1.0 °C.

Still referring to Figure 16b, the sensors positioned 1.0 m away from the wall showed virtually no temperature increase during the continuous heating phase. However, after approximately 80 hours, a warming trend was observed in the surrounding soil, with a 0.25 °C rise recorded by the sensors at 1.2 m and 3.2 m depths, which had uninterrupted data acquisition. In contrast, during the recovery phase—when the heater and pump were turned off, as shown in Figure 16c—the sensors at 1.0 m from the wall registered a temperature increase of about 1.0 °C between 96 and 200 hours, corresponding to 104 hours after the heater shutdown.

Furthermore, Figure 16c illustrates the gradual heat dissipation into the soil after the test ended. The sensors located 0.5 m from the wall recorded a 1.0 °C temperature increase between 96 and 150 hours—about 50 hours earlier than the same increase observed at 1.0 m. By 500 hours after the start of the continuous TPT, the sensors at both 0.5 m and 1.0 m distances indicated a trend toward recovering the soil's initial temperature.

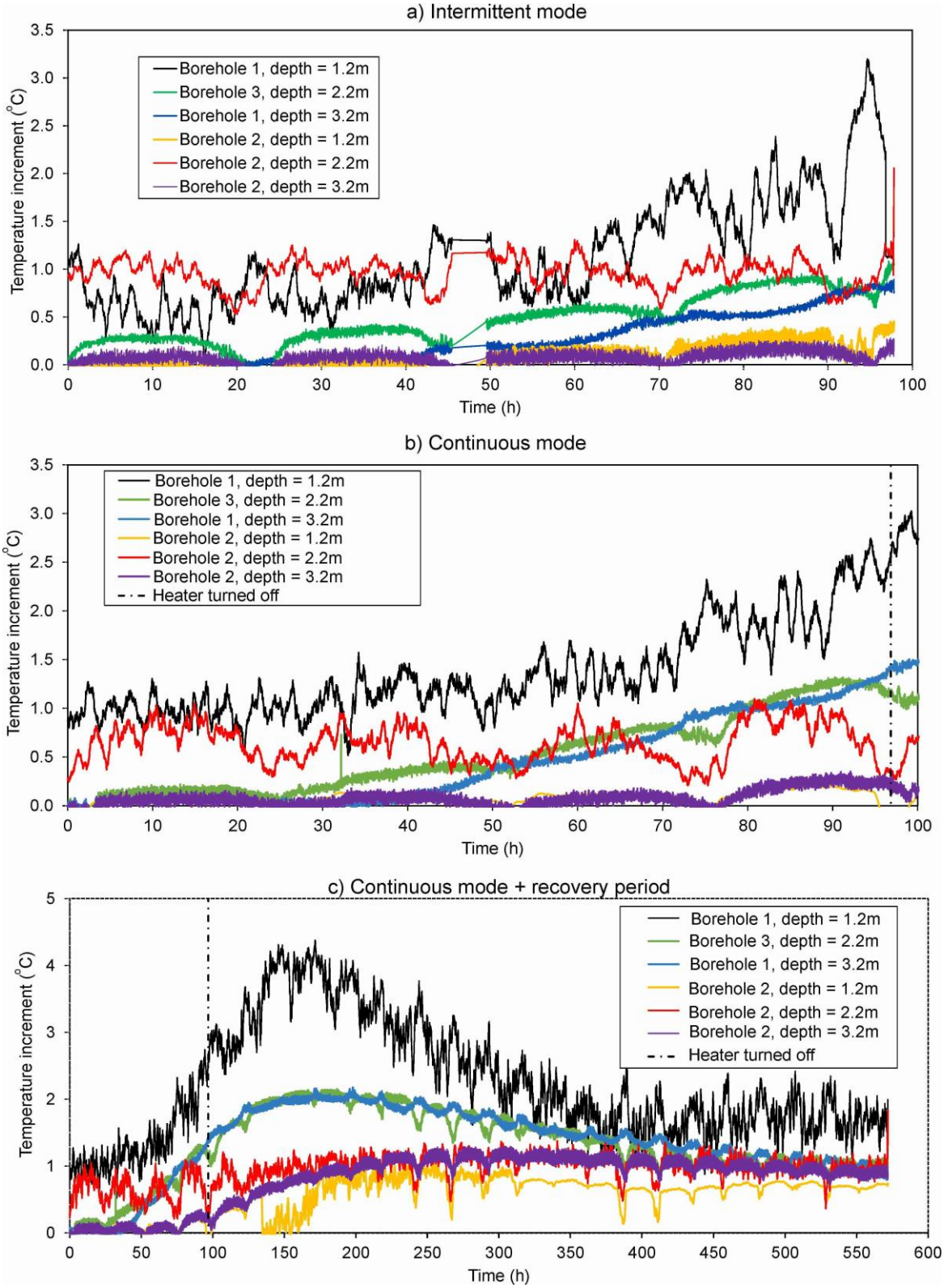

Figure 16. Soil temperature at various depths, measured by PT-100 sensors installed 0.5 m and 1.0 m away from the energy wall (Panel 4). (a) Intermittent mode; (b) Continuous mode during heating period; (c) Continuous mode during the heating test and natural recovery phases.

Between 60 and 96 hours of the TPT conducted under intermittent operation mode, a 1.0°C temperature increase was recorded by the sensor located 0.5 m from the wall at a depth of 1.2 m, which is 0.5°C lower than the increase observed in the continuous heating test. At depths of 2.2 m and 3.2 m—also 0.5 m from the wall—the temperature rise difference between the two tests remained 0.5°C during the final 30 hours: the intermittent test showed a 0.5°C increase, while the continuous test registered a 1.0°C rise. Meanwhile, sensors positioned 1.0 m from the wall recorded virtually no temperature increase throughout the four days of intermittent heating cycles. Only after the final heating cycle, at around 73 hours, the sensors at 1.2 m and 3.2 m depths (those without data acquisition issues) registered a temperature rise of nearly 0.25°C compared to the initial temperature at hour zero.

During the intermittent test shown in Figure 16a, the temperature variation in the soil at distance of 0.5 m from the wall was greater than that observed at 1.0 m. At 1.0 m, the soil showed a little temperature increase until the end of the intermittent test. On the other hand, in the continuous operation mode in Figure 16b, after 82 hours of test, the soil temperature 1.0 m away increased by 0.25°C compared to the initial time (0 h).

4.3. Heat exchange rate

A key parameter for designing energy walls is the heat exchange rate per unit area of the wall surface (q). In the thermal performance test, water circulates through the energy wall at a constant inlet temperature to transfer heat with the surrounding soil. Thus, the heat exchange rate can be determined from the inlet and outlet water temperatures and the fluid flow rate, using Equation (1). The heating-activated area considered in this study is (3 x 3.5) x 2= 21m².

The heat exchange rate per unit area of the wall surface equipped with heat exchanger pipes, obtained from the two Thermal Performance Tests (TPTs) conducted under intermittent and continuous operation modes, is presented in Figure 17. Table 4 summarizes the values heat exchange rate per unit area, *q*, for both operation modes, considering only the active periods (‘on’ cycles) during the four intermittent test cycles. The results indicate that intermittent operation may be more effective for energy walls installed in unsaturated soils under cooling demand conditions.

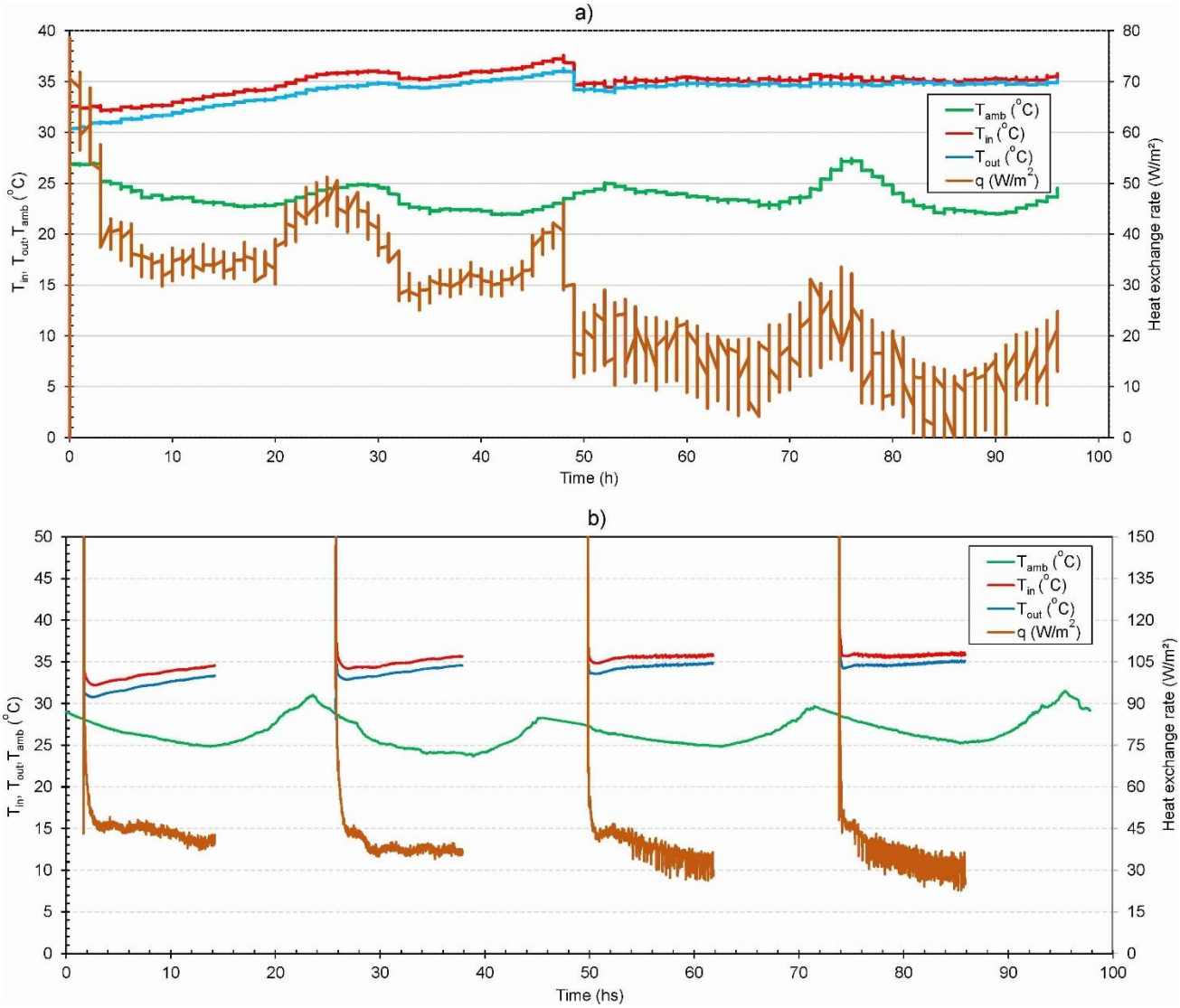

Figure 17. Heat exchange rate per unit area of wall for (a) continuous (December 2924), and (b) intermittent operation (January 2025).

The results presented in Table 4 indicate that during the first two cycles of the intermittent test and at the 10- and 34-hour marks of the continuous test, similarly high heat exchange rates per active wall area were observed. However, after 58 hours of continuous heat injection, the heat exchange rate, q, had dropped to nearly half of that recorded during intermittent operation. This decline in heat exchange efficiency is attributed to heat accumulation in the surrounding soil. As the test progressed, the intermittent operation mode consistently demonstrated a higher average heat exchange rate per active wall area compared to the continuous mode for the energy wall analysed.

Table 4. Comparison of heat exchange rate per unit wall area (W/m^2) between the intermittent and the continuous operation modes.

Energy wall panels	TPT type	(10h)	(34h)	(58h)	(82h)
4 and 5	Continuous	32	29	18	11
4 and 5	Intermittent	44	37	36	26

The thermal balance was estimated as the difference between the heat inflow and outflow, representing the net heat exchange within the system. Positive values indicate heat storage in the ground, whereas negative values correspond to heat loss, expressed in terms of power (W). As presented in Figure 18, the short-term test under the intermittent operation mode stored more heat in the ground compared to the test with continuous heat rejection over 96 hours. After 58 hours of uninterrupted heating, the soil stored only about 370 W—approximately half of the heat stored in the test with 12-hour no-heating pauses—indicating that the soil was able to partially recover its initial temperature during the pauses, i.e., resulting in enhanced heat flux and reduced thermal drift over the short-term period.

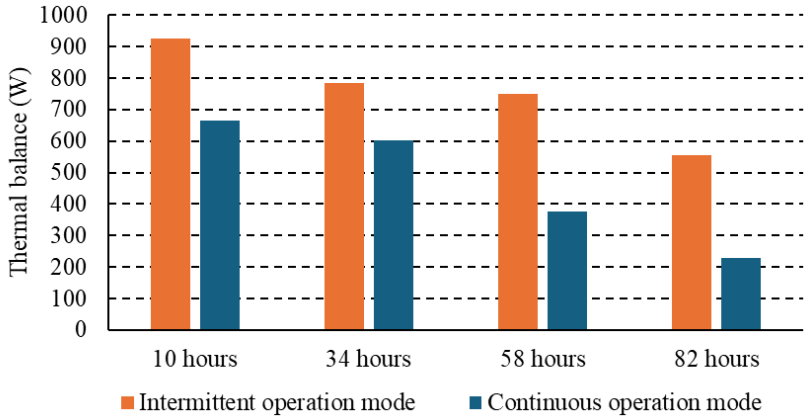

Figure 18. Thermal balance comparison between the intermittent and continuous operation mode tests.

Previous studies have highlighted the superior performance of the intermittent operation mode compared to the continuous mode in GSHP systems. Additionally, when comparing the heat exchange rate results from the short-term TPTs conducted in this study—performed on an energy wall in tropical unsaturated soil—similarities emerge with the value of 18.6 W/m² reported by [6] for building heating demand (heat extraction from the soil) under intermittent operation over a 99.6-hour test period.

Considering the natural restoration of underground temperatures when the system is not operating, the disturbed thermal conditions in the surrounding soil tend to recover during off periods. Consequently, the heat transfer performance of ground source heat pump systems can be improved through intermittent operation.

4.4. Results from Numerical and Analytical Models

The validation of numerical models and analytical models against the results from the experimental setup is crucial for analysis. Validating numerical and analytical models in cases of energy walls or any other energy geostructures ensures that the results are generalizable, can assist in optimizing operations beyond tested scenarios, and also enables the prediction of reliable output for various conditions and scale-up without costly tests through physical experimental setups.

In this study, the outlet temperatures of the fluid are used as a parameter for validation of the numerical and analytical model. The temperature input and outputs from experimental setups, along with temperature outputs from numerical and analytical models from both continuous and intermittent operations, are presented in Figures 19 and 20, respectively.

In numerical models, the thermal loads are applied through fluid flow. For both continuous and intermittent operations, the numerical models created in COMSOL Multiphysics have shown an acceptable match against the experimental setups.

In continuous operations, as soon as the thermal load is applied, a difference of about 5°C can be observed in the numerical and experimental results. However, within one hour, this difference is reduced to approximately 1°C, as seen in Figure 19. The same behaviour can be observed in the case of intermittent operations as seen in Figure 20. In intermittent operations, by the fourth day of thermal loading, the difference between numerical and experimental results shows further reduction, signifying convergence. In both cases, after a few hours, the difference between the numerical and experimental readings becomes lower than 1°C and keeps reducing with time. This shows that the initial temperature applied to the numerical models might be incorrect.

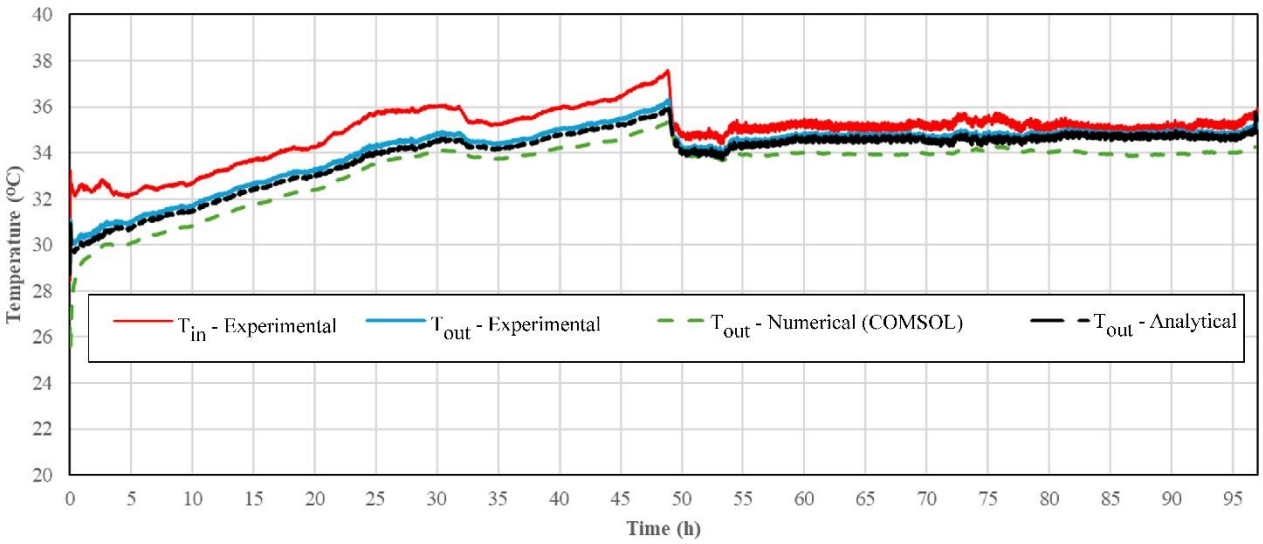

Figure 19. Fluid inlet and outlet temperatures from the continuous operation of the experimental setup and outlet temperatures from numerical and analytical models.

In terms of interpretation, the numerical model is assumed to exchange more heat with the ground when compared against the field results. Overall, the difference is less than 1°C; hence, the model predictions showed acceptable agreement with experimental data. This numerical model is validated by comparing its output temperature against experimental measurements for both intermittent and continuous operations. The model has successfully reproduced the thermal response observed in the experimental tests, hence making this model suitable for further parametric studies or as a model for testing long-term response, if needed.

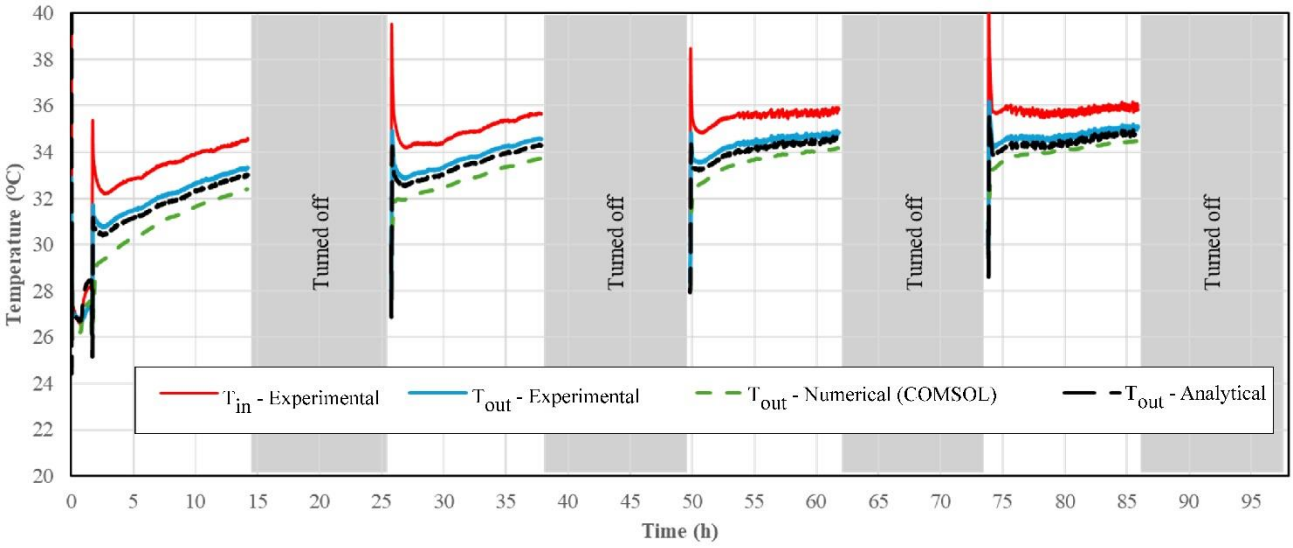

Figure 20. Fluid inlet and outlet temperatures from the intermittent operation of the experimental setup, and outlet temperatures from numerical and analytical models.

In the analytical model of the FIS Method, thermal load is applied through equivalent planar heat flux, q_p, rather than directly through fluid flow. The analytical model uses IPS as its base model and shows an acceptable match against the results from experimental setups.

For continuous operations, the difference between analytical and experimental results is mostly below 0.4°C. Moreover, after approximately 48 hours of operation, when the thermal load changes, this difference reduces even further to less than 0.2°C. This shows an excellent match against the experimental results as seen in Figure 19.

On the other hand, in case of intermittent operations, the difference between analytical temperature outputs and experimental results is below 0.4°C for the first loading cycle and reduces to below 0.35°C for the second and third loading cycles, and below 0.3°C for the fourth thermal loading cycle, as seen in Figure 20. This shows that the results of the analytical model are also converging with the experimental results.

In both modes of operation, the analytical model shows good agreement with the experimental results, indicating that the theoretical assumption and parameter estimations done in [37] represent the thermal behaviour of the current energy wall. This gives confidence to use this analytical approach for further research and practical design of energy walls with a dual pipe arrangement.

5. Conclusions

This study presents an experimental investigation into the thermal behaviour of an energy wall in contact with tropical unsaturated soil on both sides, constructed and monitored at the EESC/USP experimental site in São Carlos, Brazil. Two Thermal Performance Tests (TPTs) were conducted in the experimental program: one under continuous operation and the other under intermittent operation. These tests aimed to characterize the thermal performance of the walls and evaluate the heat exchange capacity of the surrounding unsaturated tropical soil under different operational conditions. Moreover, the results from the experimental tests were employed to construct and validate numerical and analytical models, which can subsequently be used for additional predictions.

The Thermal Performance Test (TPT) conducted under continuous operation mode, maintaining a constant inlet temperature of approximately 35 °C, resulted in an average heat exchange rate of 22.5 W/m² over 96 hours of uninterrupted heating. Throughout the test, the wall temperature progressively increased, although signs of thermal saturation appeared. The surrounding soil also experienced a temperature rise, especially in the upper layers. However, at the base of the wall (–3.5 m depth), soil temperature remained close to its initial value.

In contrast, the Thermal Performance Test (TPT) conducted under intermittent operation mode—characterized by alternating heating and recovery cycles—demonstrated improved thermal dissipation in the soil and lower wall temperatures. The average heat exchange rate reached 35.75 W/m² over the 96-hour testing period. Although this value was slightly higher than that observed in the continuous mode, heat transfer occurred more gradually, allowing better thermal recovery during the off cycles. Wall temperatures during this test ranged from 26 °C to 33 °C, while temperature increases in the surrounding soil were lower compared to the continuous heating test. These results suggest that intermittent operation may help mitigate long-term thermal accumulation around the thermoactivated structure.

Numerical and analytical models have shown a good agreement with the experimental results. For numerical and analytical models, the difference against the experimental results is generally less than 1°C and 0.4°C, respectively, for both continuous and intermittent tests. Moreover, in both numerical and analytical cases, the results were converging towards the experimental results, signifying improvement in output with time. These validated models show that these experimental results are generalizable, and these models can be used to study long-term behaviours of the models.

Overall, the experimental results show that the technical viability of energy walls in tropical unsaturated soils depends on the duration of heat rejection into the soil and the operational mode, particularly in relation to their thermal performance during the rainy summer season. The current findings can guide strategies for the use of energy wall technology in regions with unsaturated soils and high cooling demand, including alternating panel operation or implementing hybrid air-conditioning systems that integrate GSHPs with auxiliary systems.

5. Acknowledgements

The authors acknowledge the State of São Paulo Research Foundation – FAPESP and the UKRI - UK Research and Innovation /EPSRC - Engineering and Physical Sciences Research Council / UKRI - EPSRC project (Process FAPESP Nº 2022/11675-8), the National Council for Scientific and Technological Development - CNPQ for the financial support (Process 310881/2018-8), and the Coordination of Improvement of Higher Education Personnel — CAPES (for granting the master scholarship of the first author).

5. References

[1] Empresa de Pesquisa Energética – EPE, 2018. Nota Técnica EPE 030/2018 –Uso de Ar-condicionado no Setor Residencial Brasileiro: Perspectivas e contribuições para o avanço em eficiência energética (Technical Note EPE 030/2018 – Use of Air Conditioning in the Brazilian Residential Sector: Perspectives and contributions to the advancement in energy efficiency). EPE, Brasília.

[2] Loveridge F., McCartney J.S., Narsilio G. A., Sanchez M., Energy geostructures: A review of analysis approaches, in situ testing and model scale experiments, Geomechanics for Energy and the Environment, Volume 22, 100173, 2020.

[3] EPE (Empresa de Pesquisa Energética), Plano Nacional de Energia 2050–PNE 2050: Versão para consulta pública. Ministério de Minas e Energia, Empresa de Pesquisa Energética, Brasília. https://www.epe.gov.br/sites-pt/publicacoes-dados-bertos/publicacoes/PublicacoesArquivos/publicacao-227/topico-563/Relatorio%20Final%20do%20PNE%202050.pdf, 2020.

[4] Martins, N. R., & Bourne-Webb, P. J. (2021). Hybridization of heat pump systems with natural ventilation to improve energy efficiency in cooling dominated buildings. *Renewable Energy and Environmental Sustainability*, *6*, 33.

[5] Beier, R. A. (2021). Analysis of thermal response tests on boreholes with controlled inlet temperature versus controlled heat input rate. *Geothermics*, *94*, 102099.

[6] Baralis, M., & Barla, M. (2021). Development and testing of a novel geothermal wall system. *International Journal of Energy and Environmental Engineering*, *12*(4), 689-704.

[7] Barla, M., Di Donna, A., & Santi, A. (2020). Energy and mechanical aspects on the thermal activation of diaphragm walls for heating and cooling. *Renewable Energy*, *147*, 2654-2663.

[8] Di Donna, A., Loveridge, F., Piemontese, M., & Barla, M. (2021). The role of ground conditions on the heat exchange potential of energy walls. *Geomechanics for Energy and the Environment*, *25*, 100199.

[9] Brandl, H. (2006). Energy foundations and other thermo-active ground structures. *Géotechnique*, *56*(2), 81-122.

[10] Xia, C., Sun, M., Zhang, G., Xiao, S., & Zou, Y. (2012). Experimental study on geothermal heat exchangers buried in diaphragm walls. *Energy and Buildings*, *52*, 50-55.

[11] Kürten, S., Mottaghy, D., & Ziegler, M. (2015). A new model for the description of the heat transfer for plane thermo-active geotechnical systems based on thermal resistances. *Acta Geotechnica*, *10*(2), 219-229.

[12] Morais, T. D. S. O., Tsuha, C. D. H. C., Neto, L. A. B., & Singh, R. M. (2020). Effects of seasonal variations on the thermal response of energy piles in an unsaturated Brazilian tropical soil. Energy and Buildings, 216, 109971.

[13] de Freitas Murari, M. C., Tsuha, C. D. H. C., & Loveridge, F. (2022). Investigation on the thermal response of steel pipe energy piles with different backfill materials. *Renewable Energy*, *199*, 44-61.

[14] Formigari, R. C., & Tsuha, C. D. H. C. (2025). Experimental investigation on the impact of the asymmetrical heat exchange and operation modes on the thermal performance of a bored energy pile in unsaturated soil: A case study in Brazil. Geothermics, 125, 103201.

[15] Casagrande, B., Saboya Jr, F., McCartney, J. S., & Tibana, S. (2022). Investigation of a field-scale energy micropile in stratified soil under cyclic temperature changes. *Geomechanics for Energy and the Environment*, *29*, 100263.

[16] Pessin, J., & Tsuha, C. D. H. C. (2023). In-field performance of continuous flight auger (CFA) energy piles with different configurations. *Applied Thermal Engineering*, *224*, 120113.

[17] ten Bosch, S., Ravera, E., & Laloui, L. (2024). Performance of energy piles foundation in hot-dominated climate: A case study in Dubai. *Renewable Energy*, *220*, 119632.

[18] EMBRAPA (2025). Condições Meteorológicas - Estação da Embrapa Pecuária Sudeste. Energy wall and instrumentation

[19] Machado S.L., Vilar O.M. (2002). Geotechnical characteristics of an unsaturated soil deposit at São Carlos, Brazil. In Proceedings of the International Workshop on Characterisation and Engineering Properties of Natural Soil, Singapore. Balkema, Rotterdam, the Netherlands, vol. 2, 2002, pp. 1305–1321.

[20] De Mio, G. (2005). Geological conditioning aspects for piezocone test interpretation for stratigraphical identification in geotechnical and geo-environmental site investigation. *Univ. São Paulo, São Carlos, Braz.*

[21] Rocha, B. P. (2018). Geotechnical characterization of unsaturated tropical soil by in situ tests. DSc. Thesis. University of São Paulo at São Carlos School of Engineering, São Carlos, Brazil.

[22] Zacarin, J. G. M. X., Da Silva, B. O., Tsuha, C. D. H. C., & Vilar, O. M. (2023). Seasonal variation of the shaft resistance of CFA piles in unsaturated soil: a case study. *Canadian Geotechnical Journal*, *61*(1), 134-148.

[23] Bandeira Neto, L. A. (2015). An experimental study of the thermal response of heat exchanger piles in unsaturated tropical soil (Master dissertation, Universidade de São Paulo).

[24] Tarnawski, V.R., Momose, T., Leong, W.H. (2009) Assessing the impact of quartz content on the prediction of soil thermal conductivity. Geotechnique 59 (4), 331–338.

[25] Zhang, N., Yu, X., Pradhan, A., Puppala, A.J. (2015). Thermal conductivity of quartz sands by thermo-time domain reflectometry probe and model prediction. J. Mater. Civ. Eng. 27 (12), 04015059.

[26] Ewing, R. P., & Horton, R. (2007). Thermal conductivity of a cubic lattice of spheres with capillary bridges. Journal of Physics D: Applied Physics, 40(16), 4959

[27] Silva, B. O. (2025). Seasonal variability of pull-out capacity of CFA piles in unsaturated soils. Doctoral Thesis. Escola de Engenharia de São Carlos, Universidade de São Paulo, São Carlos, *in press*.

[28] Zhu, P., Wang, C., Kong, G., & Ding, X. (2024). Effects of the ground surface thermal boundary condition on the long-term thermal performance of energy diaphragm walls. *Applied Thermal Engineering*, *236*, 121865.

[29] Nogari, J. L. B. (2025). Development and evaluation of the use of a Dynamic Probing Light (DPL) adapted for determining the ground thermal conductivity in-situ (Master dissertation, Universidade de São Paulo).

776 [30] Tonus, B. P. A., Niedvieski, L. B., Lautenschläger, C. E. R., Tsuha, C.H.C., & Faro, V. P. (2024). Field and
777 laboratory estimation of thermal conductivity of unsaturated soils using thermal cone penetration test
778 (T- CPT). Environmental Earth Sciences, 83(18), 537
779 [31] Morais, T. D. S. O., Sousa, J. D., & Tsuha, C. D. H. C. (2019). Measurement of thermal conductivity of
780 unsaturated tropical soils by a needle probe method. In Geotechnical Engineering in the XXI Century:
781 Lessons learned and future challenges (pp. 2379-2387). IOS Press.
782 [32] Low, J. E., Loveridge, F. A., Powrie, W., & Nicholson, D. (2015). A comparison of laboratory and in situ
783 methods to determine soil thermal conductivity for energy foundations and other ground heat exchanger
784 applications. *Acta geotechnica*, *10*, 209-218.
785 [33] Choi, W., Kikumoto, H., Ooka, R. (2018). New perspectives in thermal performance test: cost-effective
786 apparatus and extended data analysis. Energy Build. 180, 109–121.
787 [34] Hu, S.; Kong, G.; Aboel-Naga, H.; Yang, Q. (2024). Thermomechanical response of field-scale energy wall
788 under different heating operations. Journal of Geotechnical and Geoenvironmental Engineering. 150
789 (3), 06023011.
790 [35] British Standards Institution. (2004). BS EN 1992-1-2:2004: Eurocode 2: Design of concrete structures –
791 Part 1-2: General rules – Structural fire design.
792 [36] COMSOL. (2015). *COMSOL Multipysics: Heat Transfer Module, User's Guide*. In © 1998–2018 Comsol
793 (pp. 1–702).
794 https://doc.comsol.com/5.4/doc/com.comsol.help.heat/HeatTransferModuleUsersGuide.pdf
795 [37] Gupta, A. (2024). *An analytical method to determine the amount of heat exchanged through thermally*
796 *activated embedded retaining walls*. Doctoral Thesis. University of Leeds, UK.
797 [38] Shafagh, I., Rees, S. J., Mardaras, I. U., Janó, M. C., & Carbayo, M. P. (2020). *A model of a diaphragm*
798 *wall ground heat exchanger.* Energies, 13(2). https://doi.org/10.3390/en13020300
799 [39] Sun, M., Xia, C., & Zhang, G. (2013). *Heat transfer model and design method for geothermal heat*
800 *exchange tubes in diaphragm walls.* 61, 250–259.
801 [40] Carslaw, H. S., & Jaeger, J. C. (1959). *Conduction of Heat in Solids*. Oxford University Press.
802 [41] Laloui, L., & Loria, A. F. R. (2019). *Analysis and Design of Energy Geostructures: Theoretical Essentials*
803 *and Practical Application.* In Academic Pressamic Press.

[42] Gupta, A., Loveridge, F., Shafagh, I., Tosin, B., De Hollanda, C., Tsuha, C., Neto, A. H., Guan, X., Knappett, J., & Brown, M. (2025). *Analytical validation for Energy walls with dual heat exchanger pipes.* International Conference on Energy Geotechnics 2025.